

and Au²⁺ have been discussed elsewhere.^{1,2}

Acknowledgment. Financial support by the Natural Sciences and Engineering Council of Canada (NSERC), Deutsche Forschungsgemeinschaft (DFG), and North Atlantic Treaty Organization (NATO) for a collaborative research grant to H.W. and F.A. is gratefully acknowledged.

Registry No. Au, 7440-57-5; Br₃[Au(SO₃F)₄], 72030-07-0; Au(SO₃F)₃, 36735-27-0; Au²⁺, 15456-07-2; SO₂F₂, 2699-79-8; SiF₄, 7783-61-1.

Supplementary Material Available: Experimental and simulated ESR spectra, the latter with and without quadrupole coupling (2 pages). Ordering information is given on any current masthead page.

A New Model for Dioxygen Binding in Hemocyanin. Synthesis, Characterization, and Molecular Structure of the $\mu\text{-}\eta^2\text{:}\eta^2$ Peroxo Dinuclear Copper(II) Complexes, [Cu(HB(3,5-R₂pz)₃)]₂(O₂) (R = *i*-Pr and Ph)

Nobumasa Kitajima,^{*,†} Kiyoshi Fujisawa,[†] Chisato Fujimoto,[†] Yoshihiko Moro-oka,^{*,†} Shinji Hashimoto,[†] Teizo Kitagawa,^{*,‡} Koshiro Toriumi,[†] Kazuyuki Tatsumi,^{*,§} and Akira Nakamura[§]

Contribution from the Research Laboratory of Resources Utilization, Tokyo Institute of Technology, 4259 Nagatsuta, Midori-ku, Yokohama 227, Japan, the Institute for Molecular Science, Okazaki National Institutes, Myodaiji 444, Okazaki, Japan, and the Department of Macromolecular Science, Osaka University, Toyonaka, Osaka 560, Japan.

Received May 20, 1991

Abstract: The synthesis and characterization of $\mu\text{-}\eta^2\text{:}\eta^2$ peroxo dinuclear copper(II) complexes which show many similarities to oxyhemocyanin (or oxytyrosinase) in their physicochemical properties are presented. The low-temperature reaction of a di- μ -hydroxo copper(II) complex [Cu(HB(3,5-*i*-Pr₂pz)₃)]₂(OH)₂ (**8**) with H₂O₂ gave a μ -peroxo complex [Cu(HB(3,5-*i*-Pr₂pz)₃)]₂(O₂) (**6**). Complex **6** was also prepared by dioxygen addition to a copper(I) complex Cu(HB(3,5-*i*-Pr₂pz)₃) (**9**). The preparation of an analogous peroxo complex [Cu(HB(3,5-Ph₂pz)₃)]₂(O₂) (**7**) was accomplished by the similar dioxygen treatment of a copper(I) acetone adduct Cu(Me₂CO)(HB(3,5-Ph₂pz)₃) (**10**). The reaction of **6** with CO or PPh₃ causes release of dioxygen, resulting in formation of the corresponding copper(I) adduct, Cu(CO)(HB(3,5-*i*-Pr₂pz)₃) (**11**) or Cu(PPh₃)(HB(3,5-*i*-Pr₂pz)₃) (**12**). Crystallography was performed for **6-6**(CH₂Cl₂), **8-1.5**(CH₂Cl₂), and **11**. Compound **6-6**(CH₂Cl₂) crystallizes in the monoclinic space group C2/c with *a* = 26.36 (2) Å, *b* = 13.290 (4) Å, *c* = 29.29 (2) Å, β = 114.59 (6)°, *V* = 7915 (9) Å³, and *Z* = 4. The refinement converged with the final *R* (*R*_w) value, 0.101 (0.148), for 3003 reflections with *F* ≥ 3σ(*F*_o). Compound **8-1.5**(CH₂Cl₂) crystallizes in the triclinic space group P $\bar{1}$ with *a* = 16.466 (4) Å, *b* = 16.904 (5) Å, *c* = 14.077 (3) Å, α = 112.92 (2)°, β = 99.21 (2)°, γ = 90.76 (2)°, *V* = 3550 (2) Å³, *Z* = 2, and the final *R* (*R*_w) factor, 0.083 (0.105), for 7226 reflections with *F* ≥ 3σ(*F*_o). Compound **11** crystallizes in the monoclinic space group, P2₁/*a* with *a* = 16.595 (4) Å, *b* = 19.154 (4) Å, *c* = 10.359 (2) Å, β = 106.65 (2)°, *V* = 3155 (1) Å³, *Z* = 4, and the final *R* (*R*_w) value 0.083 (0.074) for 5356 reflections with *F* ≥ 3σ(*F*_o). The X-ray analysis of **6-6**(CH₂Cl₂) definitely established the $\mu\text{-}\eta^2\text{:}\eta^2$ coordination structure of the peroxide ion for the first time. This unusual side-on structure is entirely novel for a d-block element transition-metal-dioxygen complex. Both **6** and **7** show remarkable characteristics which are very similar to those known for oxyhemocyanin and oxytyrosinase. Complex **6**: diamagnetic; ν (O–O), 741 cm⁻¹; UV–vis, 349 nm (ϵ , 21 000), 551 nm (ϵ , 790); Cu–Cu, 3.56 Å. Complex **7**: diamagnetic, ν (O–O), 759 cm⁻¹; UV–vis, 355 nm (ϵ , 18 000), 542 nm (ϵ , 1040). These properties are all consistent with those of an analogous complex, [Cu(HB(3,5-Me₂pz)₃)]₂(O₂) (**5**), of which the characterization and reactivities were reported already (Kitajima, N., et al. *J. Am. Chem. Soc.* **1990**, *112*, 6402; **1991**, *113*, 5664). The magnetic and spectroscopic features of **5-7** and their biological relevance are discussed in detail. Furthermore, simple interpretation of the electronic state of the N₃Cu(O₂²⁻)CuN₃ chromophore is provided based on extended Hückel MO calculations. The close resemblance between the properties of $\mu\text{-}\eta^2\text{:}\eta^2$ peroxo complexes **5-7** and oxyhemocyanin led us to propose a new model for dioxygen binding in hemocyanin; dioxygen is simply bound between the two copper ions in the $\mu\text{-}\eta^2\text{:}\eta^2$ mode. With this structural model; the existence of an endogenous bridging ligand, which has been generally supposed to account for the diamagnetism of oxyhemocyanin, is no longer necessary.

Introduction

Hemocyanin (Hc) is a ubiquitous oxygen transport protein for invertebrates: arthropods and molluscs.¹⁻³ Hc contains a dinuclear copper site with a Cu–Cu separation of ca. 3.6 Å.^{4,5} Dioxygen is known to bind to this site as a peroxide ion in a symmetric coordination mode.⁶⁻⁸ Accordingly, the valence change of the copper ions is interpreted in terms of a two-electron oxidation: Cu(I,I) in deoxy-Hc and Cu(II,II) in oxy-Hc. A striking feature of oxy-Hc is its diamagnetism due to the strong antifer-

romagnetic coupling between the two copper(II) ions ($-2J > 600$ cm⁻¹).^{9,10} Furthermore, instead of the weak d–d transitions at

(1) *Structure and Function of Hemocyanin*; Bannister, J. V., Ed.; Springer-Verlag: Berlin, Heidelberg, New York 1977.

(2) Solomon, E. I.; Penfield, K. W.; Wilcox, D. E. *Struct. Bonding (Berlin)* **1983**, *53*, 1–57.

(3) Solomon, E. I. *Metal Clusters in Proteins*; Que, L., Jr., Ed.; ACS Symposium Series 372, American Chemical Society: Washington, D.C., 1988; pp 116–150.

(4) (a) Gaykema, W. P. J.; Hol, W. G. J.; Vereijken, J. M.; Soeter, N. M.; Bak, H. J.; Beintema, J. J. *Nature* **1984**, *309*, 23–29. (b) Gaykema, W. P. J.; Volbeda, A.; Hol, W. G. J. *J. Mol. Biol.* **1985**, *187*, 255–275.

(5) (a) Volbeda, A.; Hol, W. G. J. *J. Mol. Biol.* **1989**, *206*, 531–546. (b) Volbeda, A.; Hol, W. G. J. *J. Mol. Biol.* **1989**, *209*, 249–279.

[†] Tokyo Institute of Technology.

[‡] Institute of Molecular Science.

[§] Osaka University.

600–700 nm normally observed for copper(II) compounds, oxy-Hc exhibits two intense absorption bands at ca. 350 and 580 nm. Tyrosinase (Tyr),¹¹ the oldest known monooxygenase which catalyzes aerobic oxidation of phenol to quinone, also contains a dicopper site and forms a stable peroxide adduct oxy-Tyr of which the properties are extremely similar to those of oxy-Hc.^{12–14} Because of their unusual properties, the structural elucidation of oxy-Hc and oxy-Tyr has been the focus of numerous physicochemical investigations in recent years. Generally, the peroxide ion is suggested to be bound at the dicopper site in a *cis-μ-1,2* coordination mode, along with an unknown endogenous bridging ligand.

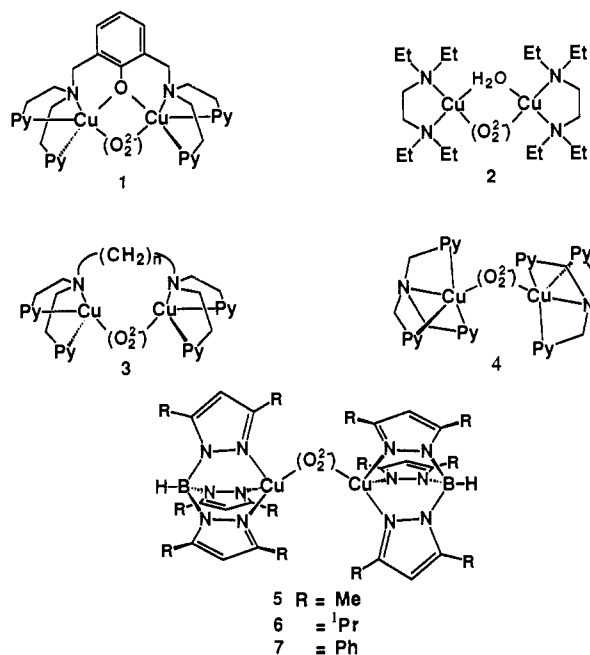
The striking characteristics of oxy-Hc and oxy-Tyr have also fascinated many inorganic chemists, and the synthesis and characterization of *μ-1,2* peroxo dinuclear copper(II) complexes, modeling the active site of oxy-Hc and oxy-Tyr, has been a current topic in bioinorganic chemistry.^{15,16} A few dinuclear copper(I) complexes^{17–19} were demonstrated to bind dioxygen reversibly; however, the dioxygen adducts were not stable enough to be characterized by adequate spectroscopic means, and thus there is some debate as to whether the formed species was certainly a peroxo complex.

The first solid evidence for the formation of a peroxo dinuclear copper complex appeared in 1984 when Karlin et al. reported the synthesis of a dinuclear copper(I) complex by use of a dinucleating ligand containing a bridging phenoxo group.²⁰ It was demonstrated that the complex reacts with dioxygen quasireversibly, affording a peroxo dinuclear copper(II) complex (**1**) based on the O–O stretching vibration frequency (803 cm⁻¹) determined by resonance Raman spectroscopy. The subsequent detailed Raman study,²¹ however, led to the conclusion that the peroxide ion is coordinated in an unsymmetric terminal fashion different from the mode suggested for oxy-Hc. In 1984, Thompson also reported the synthesis of a *μ*-peroxo dinuclear copper(II) complex (**2**) by dioxygen treatment of the copper(I) ethylene complex with *N,N,N',N'*-tetraethylethylenediamine.²² The assignment of the

Table I. Bond Distances (Å) and Angles (deg) for [Cu(HB(3,5-*i*-Pr₂pz)₃)]₂(OH)₂-1.5(CH₂Cl₂) (8-1.5(CH₂Cl₂))

Distances			
Cu1–O1	1.953 (6)	Cu1–O2	1.934 (5)
Cu1–N1	2.371 (6)	Cu1–N2	2.016 (6)
Cu1–N3	2.010 (8)	Cu2–O1	1.921 (5)
Cu2–O2	1.946 (7)	Cu2–N4	2.640 (7)
Cu2–N5	1.984 (7)	Cu2–N6	1.989 (6)
Cu1–Cu2	2.937 (2)		
Angles			
O1–Cu1–O2	79.2 (2)	N1–Cu1–O1	119.7 (3)
N1–Cu1–O2	89.1 (2)	N2–Cu1–O1	94.7 (3)
N2–Cu1–O2	173.8 (3)	N3–Cu1–O1	155.2 (3)
N3–Cu1–O2	97.4 (3)	N1–Cu1–N2	93.4 (2)
N1–Cu1–N3	84.6 (3)	N2–Cu1–N3	88.5 (3)
O1–Cu2–O2	79.6 (2)	N4–Cu2–O1	80.9 (2)
N4–Cu2–O2	117.3 (2)	N5–Cu2–O1	95.6 (2)
N5–Cu2–O2	160.2 (3)	N6–Cu2–O1	171.7 (3)
N6–Cu2–O2	98.3 (3)	N4–Cu2–N5	80.4 (3)
N4–Cu2–N6	93.1 (2)	N5–Cu2–N6	89.0 (3)

structure was based solely on the IR spectrum, and, unfortunately, the details of the structure and properties of the complex have not been provided.



(6) (a) Freedman, T. B.; Loehr, J. S.; Loehr, T. M. *J. Am. Chem. Soc.* **1976**, *98*, 2809–2815. (b) Thamann, T. J.; Loehr, J. S.; Loehr, T. M. *J. Am. Chem. Soc.* **1977**, *99*, 4187–4189.

(7) Larrabee, J. A.; Spiro, T. G. *J. Am. Chem. Soc.* **1980**, *102*, 4217–4223.

(8) Loehr, T. M. *Oxygen Complexes and Oxygen Activation by Transition Metals*, Martell, A. E., Sawyer, D. T., Eds.; Plenum: New York, 1988; pp 17–32.

(9) Moss, T. H.; Gould, D. C.; Ehrenberg, A.; Loehr, J. S.; Mason, H. S. *Biochemistry* **1973**, *12*, 2444–2449.

(10) (a) Solomon, E. I.; Dooley, D. M.; Wang, R. H.; Gray, H. B.; Cerdonio, M.; Mogno, F.; Romani, G. L. *J. Am. Chem. Soc.* **1976**, *98*, 1029–1031. (b) Dooley, D. M.; Scott, R. A.; Ellinghaus, J.; Solomon, E. I.; Gray, H. B. *Proc. Natl. Acad. Sci. U.S.A.* **1978**, *75*, 3019–3022.

(11) Mason, H. S.; Fowls, W. B.; Peterson, E. W. *J. Am. Chem. Soc.* **1955**, *77*, 2914–2915.

(12) Jolley, R. L., Jr.; Evans, L. H.; Makino, N.; Mason, H. S. *J. Biol. Chem.* **1974**, *249*, 335–345.

(13) Eickman, N. C.; Solomon, E. I.; Larrabee, J. A.; Spiro, T. G.; Lerch, K. *J. Am. Chem. Soc.* **1978**, *100*, 6529–6531.

(14) Himmelwright, R. S.; Eickman, N. C.; LuBien, C. D.; Lerch, K.; Solomon, E. I. *J. Am. Chem. Soc.* **1980**, *102*, 7339–7344.

(15) (a) Karlin, K. D.; Gultneh, Y. *Prog. Inorg. Chem.* **1987**, *35*, 219–327. (b) Tyeklar, Z.; Karlin, K. D. *Acc. Chem. Res.* **1989**, *22*, 241–248.

(16) Sorrell, T. N. *Tetrahedron* **1989**, *45*, 3–68.

(17) Bulkowski, J. E.; Burk, P. L.; Ludmann, M.-F.; Osborn, J. A. *J. Chem. Soc., Chem. Commun.* **1977**, 498–499.

(18) (a) Simmons, M. G.; Wilson, L. J. *J. Chem. Soc., Chem. Commun.* **1978**, 634–636. (b) Merrill, C. L.; Wilson, L. J.; Thamann, T. J.; Loehr, T. M.; Ferris, N. S.; Woodruff, W. H. *J. Chem. Soc., Dalton Trans.* **1984**, 2207–2221.

(19) Nishida, Y.; Takahashi, K.; Kuramoto, H.; Kida, S. *Inorg. Chim. Acta* **1981**, *54*, L103–L104.

(20) (a) Karlin, K. D.; Cruse, R. W.; Gultneh, Y.; Hayes, J. C.; Zubieta, J. *J. Am. Chem. Soc.* **1984**, *106*, 3372–3374. (b) Karlin, K. D.; Cruse, R. W.; Gultneh, Y.; Farooq, A.; Hayes, J. C.; Zubieta, J. *J. Am. Chem. Soc.* **1987**, *109*, 2668–2679.

(21) Pate, J. E.; Cruse, R. W.; Karlin, K. D.; Solomon, E. I. *J. Am. Chem. Soc.* **1987**, *109*, 2624–2630.

(22) Thompson, J. S. *J. Am. Chem. Soc.* **1984**, *106*, 8308–8309.

Karlin and co-workers further succeeded in preparing two other structurally distinct *μ*-peroxo dinuclear copper complexes (**3** and **4**). The coordination structure of **3** was suggested to be *cis-μ-1,2* or *μ-η²:η²* based on an EXAFS analysis.^{23,24} Interestingly, **3** mimics, to a certain extent, the absorption spectroscopic features and magnetic properties of oxy-Hc. The O–O vibration frequency in **3** was not ascertained, however, because of its instability under the laser excitation conditions.²³ The structure of **4** was definitely established by X-ray crystallography as *trans-μ-1,2*,²⁵ yet, the spectroscopic properties of the complex are apparently different from those of oxy-Hc, thereby providing negative evidence that oxy-Hc does not possess a *trans-μ-1,2* coordination mode.

Consequently, a structurally well-defined system that mimics the characteristics of oxy-Hc and oxy-Tyr in its physicochemical properties was not developed until the synthesis and characteri-

(23) (a) Karlin, K. D.; Haka, M. S.; Cruse, R. W.; Gultneh, Y. *J. Am. Chem. Soc.* **1985**, *107*, 5828–5829. (b) Karlin, K. D.; Haka, M. S.; Cruse, R. W.; Meyer, G. J.; Farooq, A.; Gultneh, Y.; Hayes, J. C.; Zubieta, J. *J. Am. Chem. Soc.* **1988**, *110*, 1196–1207.

(24) Blackburn, N. J.; Strange, R. W.; Farooq, A.; Haka, M. S.; Karlin, K. D. *J. Am. Chem. Soc.* **1988**, *110*, 4263–4272.

(25) Jacobson, R. R.; Tyeklar, Z.; Farooq, A.; Karlin, K. D.; Liu, S.; Zubieta, J. *J. Am. Chem. Soc.* **1988**, *110*, 3690–3692.

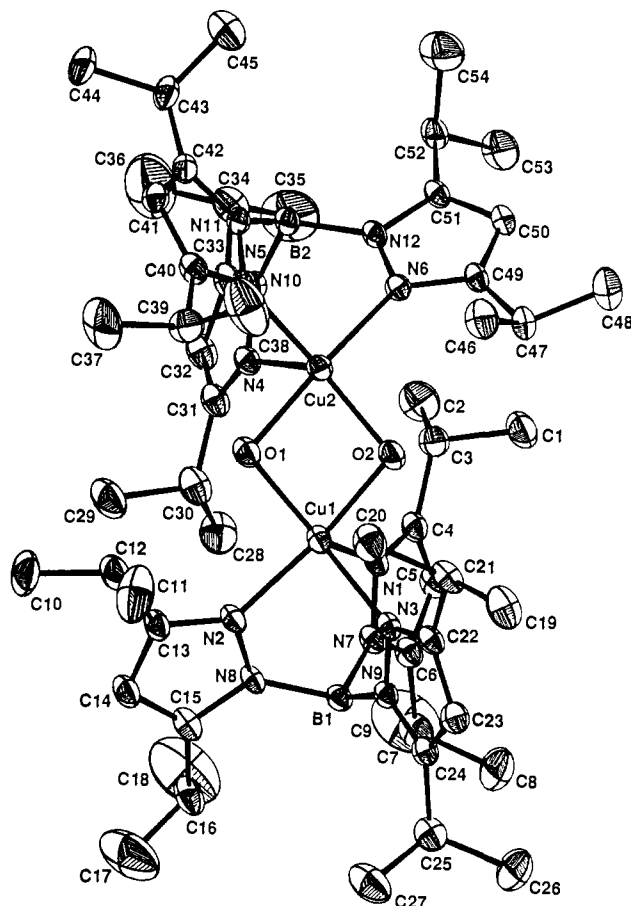


Figure 1. ORTEP view of $[\text{Cu}(\text{HB}(3,5\text{-}i\text{-Pr}_2\text{pz})_3)_2(\text{OH})_2]$ (**8**) (30% probability). CH_2Cl_2 molecules of crystallization were omitted for clarity.

zation of $\mu\text{-}\eta^2\text{:}\eta^2$ peroxo dinuclear copper(II) complexes ligated by tris(pyrazolyl)borate ligands (**5**–**7**) reported by Kitajima et al.^{26,27} These peroxo complexes do not contain a bridging ligand other than the peroxide ion, and they exhibit the remarkable characteristics as follows: (1) diamagnetic, (2) $\nu(\text{O}=\text{O})$ stretching frequencies observed at $725\text{--}760\text{ cm}^{-1}$, (3) a symmetric coordination mode of the peroxide ion as in oxy-Hc established by resonance Raman spectroscopy, (4) characteristic absorption bands appearing at ca. 350 (ϵ , $20\,000$) and ca. 550 nm (ϵ , 1000), (5) absence of the Raman band assignable to Cu–O stretching vibration with 514.5-nm excitation, and (6) Cu–Cu separation of ca. 3.6 \AA .^{26,27,29} All these properties are very similar to those known for oxy-Hc and oxy-Tyr,¹ raising a new possibility that oxy-Hc contains the same particular coordination mode, $\mu\text{-}\eta^2\text{:}\eta^2$. The synthesis and reactivity of $[\text{Cu}(\text{HB}(3,5\text{-Me}_2\text{pz})_3)_2(\text{O}_2)]$ (**5**) have been reported previously.^{28,29} In the present paper, the synthesis and characterization of **6** and **7**, crystal structure of **6**, and simple interpretations of the electronic structure of the $\text{N}_3\text{Cu}(\mu\text{-}\eta^2\text{:}\eta^2\text{-O}_2^2\text{-})\text{CuN}_3$ chromophore based on the extended Hückel MO calculations are provided. A preliminary account of the study on **6** was reported earlier as a communication.²⁷

Results and Discussion

Synthesis and Structure of di- μ -Hydroxo Dinuclear Complex (8**).** Treatment of $\text{Cu}(\text{Br})(\text{HB}(3,5\text{-}i\text{-Pr}_2\text{pz})_3)$ with 1 N aqueous NaOH solution in toluene yields a di- μ -hydroxo copper(II) complex (**8**).³⁰ Recrystallization from CH_2Cl_2 gave X-ray quality

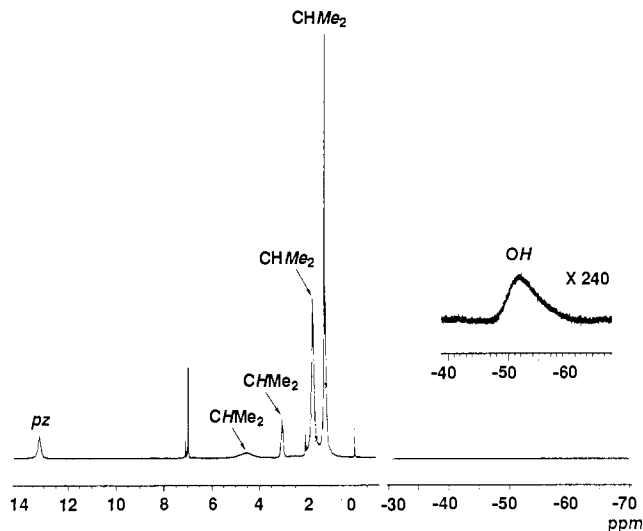
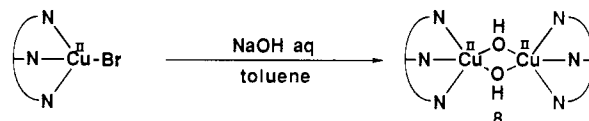


Figure 2. 270 MHz ^1H NMR spectrum of $[\text{Cu}(\text{HB}(3,5\text{-}i\text{-Pr}_2\text{pz})_3)_2(\text{OH})_2]$ (**8**) in toluene- d_8 at $-40\text{ }^\circ\text{C}$.

crystals of **8** solvated with CH_2Cl_2 ($8 \cdot 1.5(\text{CH}_2\text{Cl}_2)$). The crystal structure of **8** is presented in Figure 1, and selected bond lengths and bond angles are summarized in Table I. There is no crystallographically required symmetry in the molecule. Two $[\text{Cu}(\text{HB}(3,5\text{-}i\text{-Pr}_2\text{pz})_3)]^+$ units are bridged by two hydroxo groups to form a dinuclear structure. All Cu–O bond lengths are similar to one another and located in the range typical for Cu–OH bonds. The coordination arrangement of each copper is best described as tetragonal with a basal plane formed by two oxygen atoms from the hydroxo groups and two pyrazole nitrogen atoms from the tris(pyrazolyl)borate ligand. The two apical pyrazole nitrogen atoms (N1 and N4) assume a cis configuration relative to one another with mean bond distances from the copper ion of 2.371 (**6**) and 2.640 (**7**) \AA , respectively. This structural feature is clearly distinct from the analogous complex $[\text{Cu}(\text{HB}(3,5\text{-Me}_2\text{pz})_3)_2(\text{OH})_2]$, which possesses a crystallographically imposed center of symmetry, requiring the two apical nitrogen atoms to be in a trans configuration.²⁹ The Cu–Cu separation in **8** is 2.937 (**2**) \AA , which is slightly shorter than the distance of 3.059 (**2**) \AA found in $[\text{Cu}(\text{HB}(3,5\text{-Me}_2\text{pz})_3)_2(\text{OH})_2]$.



In accord with its doubly bridged dinuclear structure, **8** exhibits antiferromagnetic properties. A frozen solution of **8** in liquid nitrogen is EPR silent, whereas it does give rise to a characteristic ^1H NMR spectrum which is given in Figure 2. The spectrum was recorded at $-40\text{ }^\circ\text{C}$. The signal assigned to the proton on the pyrazole ring appears at 13.2 ppm , which is considerably down-shifted from the values for diamagnetic copper(I) complexes ($5.7\text{--}6.1\text{ ppm}$).³¹ A very broad signal is observed at -52 ppm , which is assignable to the bridging hydroxo group, because the signal disappeared when D_2O was added. As we reported previously,²⁹ $[\text{Cu}(\text{HB}(3,5\text{-Me}_2\text{pz})_3)_2(\text{OH})_2]$ is in equilibrium with a μ -oxo complex $[\text{Cu}(\text{HB}(3,5\text{-Me}_2\text{pz})_3)_2\text{O}]$ in CHCl_3 .³² However, no evidence was acquired for such a conversion of **8** to a μ -oxo dinuclear complex; in fact, the IR spectrum of **8** in CHCl_3 shows a band assignable to $\nu(\text{OH})$ (3622 cm^{-1}), and treatment of **8** with an excess amount PPh_3 does not give any detectable amount of OPPh_3 , whereas the μ -oxo complex $[\text{Cu}(\text{HB}(3,5\text{-Me}_2\text{pz})_3)_2\text{O}]$ generated from $[\text{Cu}(\text{HB}(3,5\text{-Me}_2\text{pz})_3)_2(\text{OH})_2]$ in CHCl_3 oxidizes

(26) Kitajima, N.; Koda, T.; Hashimoto, S.; Kitagawa, T.; Moro-oka, Y. *J. Chem. Soc., Chem. Commun.* **1988**, 151–152.

(27) Kitajima, N.; Fujisawa, K.; Moro-oka, Y.; Toriumi, K. *J. Am. Chem. Soc.* **1989**, *111*, 8975–8976.

(28) Kitajima, N.; Koda, T.; Iwata, Y.; Moro-oka, Y. *J. Am. Chem. Soc.* **1990**, *112*, 8833–8839.

(29) Kitajima, N.; Koda, T.; Hashimoto, S.; Kitagawa, T.; Moro-oka, Y. *J. Am. Chem. Soc.* **1991**, *113*, 5664–5671.

(30) Kitajima, N.; Fujisawa, K.; Moro-oka, Y. *Inorg. Chem.* **1990**, *29*, 357–358.

(31) Kitajima, N.; Fujisawa, K.; Fujimoto, C.; Moro-oka, Y. *Chem. Lett.* **1989**, 421–424.

(32) Kitajima, N.; Koda, T.; Moro-oka, Y. *Chem. Lett.* **1988**, 347–350.

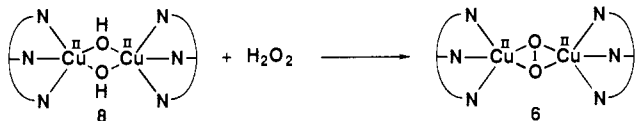
Table II. Bond Distances (Å) and Angles (deg) for [Cu(HB(3,5-*i*-Pr₂pz)₃)₂(O₂)-6(CH₂Cl₂)] (6-6(CH₂Cl₂))

Distances			
Cu-O	1.903 (11)	Cu-O'	1.927 (9)
Cu-N1	2.000 (8)	Cu-N2	2.258 (8)
Cu-N3	1.993 (14)	B-N4	1.55 (2)
B-N5	1.53 (2)	B-N6	1.58 (2)
N1-N4	1.382 (14)	N2-N5	1.391 (14)
N3-N6	1.417 (14)	O-O'	1.412 (12)
Cu-Cu'	3.560 (3)		

Angles			
O-Cu-O'	43.3 (4)	O-Cu-N1	107.2 (4)
O-Cu-N2	114.2 (4)	O-Cu-N3	150.4 (4)
O'-Cu-N1	148.8 (4)	O'-Cu-N2	111.5 (4)
O'-Cu-N3	111.3 (4)	N1-Cu-N2	88.5 (3)
N1-Cu-N3	92.7 (4)	N2-Cu-N3	87.4 (4)
Cu-N1-N4	118.4 (6)	Cu-N2-N5	111.0 (6)
Cu-N3-N6	118.9 (7)	N4-B-N5	110.6 (12)
N4-B-N6	108.1 (8)	N5-B-N6	111.4 (9)
B-N4-N1	118.0 (8)	B-N5-N2	120.9 (7)
B-N6-N3	115.8 (11)		

PPh₃ to OPPh₃ quantitatively. Therefore, it is conclusive that the di- μ -hydroxo structure of **8** is preserved in solution.

Synthesis and Structure of μ -Peroxo Dinuclear Copper(II) Complex 6. In an analogous manner applied to the preparation of [Cu(HB(3,5-Me₂pz)₃)₂(O₂) (**5**),^{26,29} low-temperature treatment of **8** with H₂O₂ affords a μ -peroxo dinuclear copper(II) complex (**6**). Addition of an excess of H₂O₂ (35 wt% aqueous solution) to a CH₂Cl₂ solution of **8** under argon at -50 °C causes a color change of the solution from blue to deep purple within 20 min. Cooling of the solution at -78 °C, affords **6**, solvated with CH₂Cl₂,



as a purple precipitate. Complex **6** is thermally unstable, but, below -10 °C in noncoordinating solvents, it is reasonably stable under Ar.

Complex **6** is also obtainable by direct dioxygen addition to a copper(I) complex **9**, which is prepared by the reaction of CuCl with KHB(3,5-*i*-Pr₂pz)₃ in acetone as a very air-sensitive product. The elemental analysis and ¹H NMR are consistent with the formulation of **9** as [Cu(HB(3,5-*i*-Pr₂pz)₃)_n]; the complex does not contain coordinated acetone based on the IR spectrum. With a less hindered tris(pyrazolyl)borate ligand HB(3,5-Me₂pz)₃, a similar complex has been reported, and the structure was determined by X-ray crystallography as a dimer, [Cu(HB(3,5-Me₂pz)₃)₂].³³ However, because of the higher steric hindrance of the present ligand and the high reactivity experimentally observed (vide infra), we suggest that **9** is a monomeric three-coordinate copper(I) complex ([Cu(HB(3,5-Me₂pz)₃)]₂ is not very reactive toward dioxygen; the complex reacts with dioxygen slowly in CHCl₃, to give Cu[HB(3,5-Me₂pz)₃]₂.³⁴ Here, it is noteworthy that each copper(I) ion in deoxy-Hc is also three-coordinate with a N₃ ligand donor set; the X-ray analysis of deoxy-Hc^{4,5} revealed that each copper(I) ion is supported with three histidyl nitrogen atoms from the protein chains, although the resolution may not be high enough to exclude the possibility that an endogenous ligand (most likely OH⁻) sits between the two copper ions, rendering the copper(I) ions four-coordinate.

When **9** was stirred under 1 atm of O₂ for 1 h at -78 °C in acetone, the slight yellow color of the solution changed to deep purple. The O₂ uptake at this stage, determined manometrically, was 0.5 per mol of **9**, confirming quantitative formation of **6** from **9**. In noncoordinating solvents, e.g., CHCl₃ and CH₂Cl₂, the

(33) Mealli, C.; Arcus, C. S.; Wilkinson, J. L.; Marks, T. J.; Ibers, J. A. *J. Am. Chem. Soc.* **1976**, *98*, 711-718.

(34) Kitajima, N.; Moro-oka, Y.; Uchida, A.; Sasada, Y.; Ohashi, Y. *Acta Crystallogr.* **1988**, *C44*, 1876-1878.

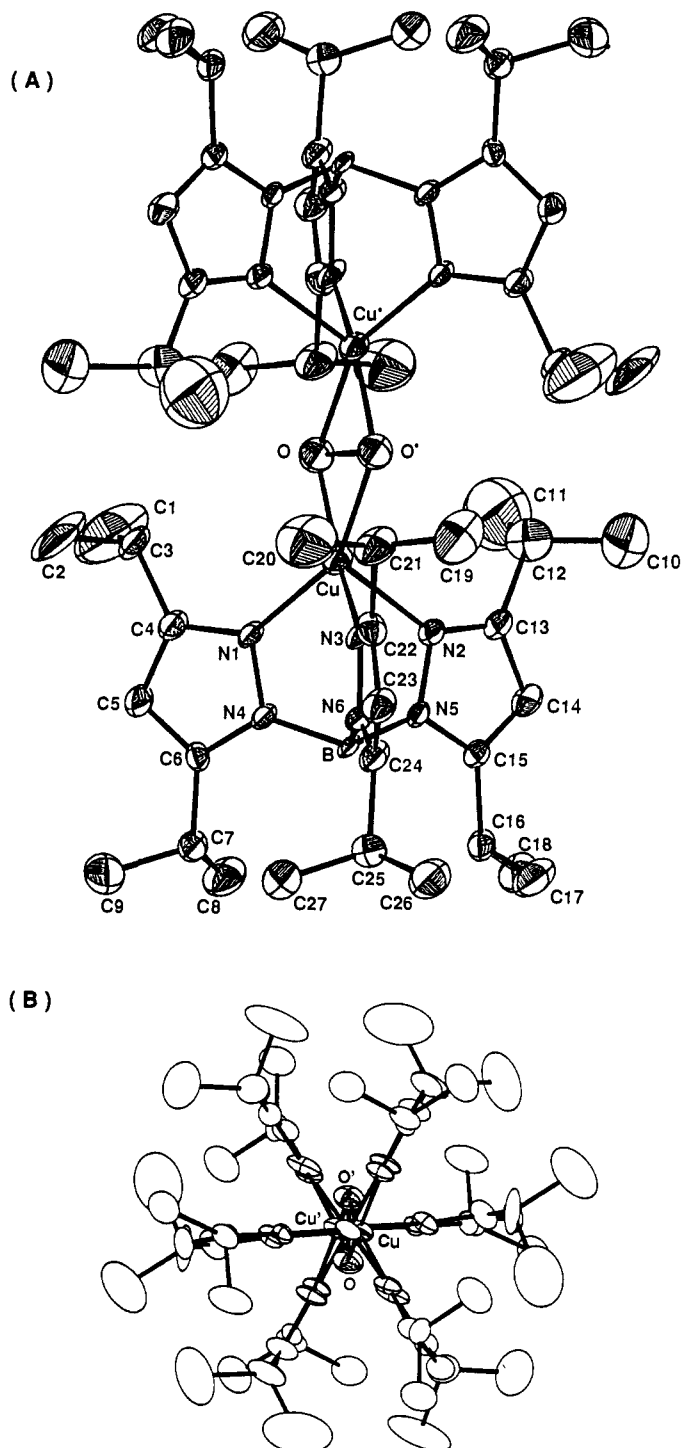


Figure 3. (A) ORTEP view of [Cu(HB(3,5-*i*-Pr₂pz)₃)₂(O₂) (**6**) (30% probability). The molecule sits on the center of symmetry. CH₂Cl₂ molecules of crystallization were omitted for clarity. (B) View of **6** looking down the B-B' axis.

reaction is very fast even at -78 °C, and isolation of **6** cannot be effected due to the fast formation of a paramagnetic green complex whose structure has not been clarified yet. On the other hand, in a strongly coordinating solvent such as DMF, the dioxygen addition is very slow.



Slow recrystallization of **6** from CH₂Cl₂ at low temperature gave X-ray quality crystals of 6-6(CH₂Cl₂). Given in Figures 3

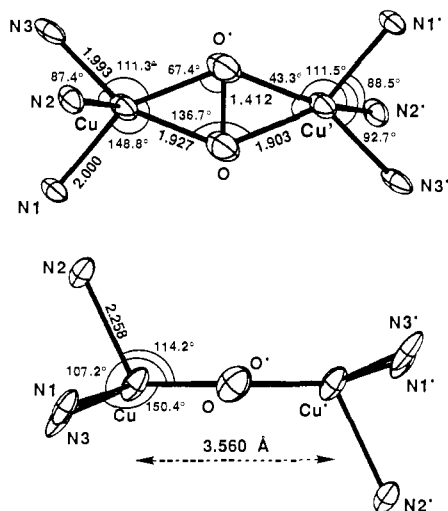


Figure 4. Expanded view of the copper coordination sphere for the molecule $[\text{Cu}(\text{HB}(3,5\text{-}i\text{-Pr}_2\text{pz})_3)_2(\text{O}_2)]$ (**6**).

and **4** are ORTEP views of the molecule **6** and the expanded view of the $\text{N}_3\text{Cu}(\text{O}_2)\text{CuN}_3$ moiety, respectively. Selected bond distances and angles and atomic coordinates are provided in Tables II and III, respectively. The molecule sits on a crystallographically imposed center of symmetry; two $[\text{Cu}(\text{HB}(3,5\text{-}i\text{-Pr}_2\text{pz})_3)]^+$ units are bridged by a peroxide ion, forming the dinuclear structure. The O–O distance (1.412 (12) Å) is located in the range typical for a peroxide ion bound to a transition-metal ion.⁶⁸ In addition to the center of symmetry, the molecule has a noncrystallographic pseudo- C_{3v} axis along B–B' as shown in Figure 3 at the bottom (as the molecule view (B)). Thus, the six isopropyl groups form a cage-like space, in which the peroxide ion is effectively encapsulated. All the Cu–O bond lengths are equivalent within experimental error, clearly establishing the unusual side-on coordination mode of the peroxide ion described as $\mu\text{-}\eta^2\text{:}\eta^2$. The $\mu\text{-}\eta^2\text{:}\eta^2$ structure is entirely novel for a peroxo complex of a d-block element, although such a coordination mode has been suggested for several complexes,^{35,36} including a copper complex.²⁴

Two of the Cu–N distances (2.000 (8) and 1.993 (14) Å) are short and almost identical to the Cu–O distances, whereas the other Cu–N bond length is considerably longer (2.258 (8) Å). Therefore, the ligand arrangement can be described as square-pyramidal, although the geometry is very distorted. The basal plane consists of two oxygen atoms from the peroxide ion and two nitrogen atoms from the tris(pyrazolyl)borate ligand, while the other pyrazole nitrogen atom is regarded as an apical ligand.

Two examples of $\mu\text{-}\eta^2\text{:}\eta^2$ peroxo dinuclear complexes of f-block elements (La^{37} and U^{38}) are known, the unusual coordination structure interpreted to be based on the high oxophilicity of these f-element transition-metal ions. However, this explanation cannot be applied for **6**, since the oxophilicity of copper(II) ion is not markedly high in general. Rather, we ascribe the $\mu\text{-}\eta^2\text{:}\eta^2$ structure found in **6** to the strong peculiarity of copper(II) ion to favor a five-coordinate structure over tetrahedral coordination. Given the coordination mode of the peroxide ion as trans- $\mu\text{-}1,2$ or cis- $\mu\text{-}1,2$, a tetrahedral geometry is required for the copper coordination structure, which is not preferable for copper(II) ion (a tetragonal geometry is unavailable with the present hindered, rigid tripodal ligands). It is possible to prepare isolable tetrahedral complexes $\text{Cu}(\text{X})(\text{HB}(3,5\text{-}i\text{-Pr}_2\text{pz})_3)^{39,40}$ (where X is a mono-

Table III. Atomic Coordinates for $[\text{Cu}(\text{HB}(3,5\text{-}i\text{-Pr}_2\text{pz})_3)_2(\text{O}_2)]\cdot 6\text{-}6(\text{CH}_2\text{Cl}_2)$ (**6**- $6(\text{CH}_2\text{Cl}_2)$)

atom	x/a	y/b	z/c
Cu	0.2318 (1)	0.1818 (1)	0.0449 (1)
O	0.2558 (4)	0.2038 (5)	-0.0094 (3)
N1	0.2121 (5)	0.0351 (6)	0.0455 (3)
N2	0.3181 (5)	0.1608 (6)	0.1200 (3)
N3	0.1785 (6)	0.2179 (6)	0.0827 (3)
N4	0.2106 (5)	-0.0053 (6)	0.0855 (3)
N5	0.3007 (4)	0.1020 (6)	0.1518 (3)
N6	0.1797 (5)	0.1532 (6)	0.1216 (3)
B	0.2303 (7)	0.0636 (9)	0.1353 (4)
C1	0.2321 (19)	-0.1000 (19)	-0.0508 (9)
C2	0.1120 (12)	-0.0396 (24)	-0.0792 (6)
C3	0.1867 (8)	-0.0257 (9)	-0.0419 (4)
C4	0.1926 (7)	-0.0403 (8)	0.0111 (4)
C5	0.1797 (7)	-0.1259 (9)	0.0325 (4)
C6	0.1910 (5)	-0.1019 (7)	0.0813 (4)
C7	0.1862 (7)	-0.1684 (8)	0.1207 (4)
C8	0.2510 (8)	-0.2208 (11)	0.1518 (5)
C9	0.1308 (9)	-0.2453 (12)	0.0958 (6)
C10	0.4703 (13)	0.3166 (18)	0.1623 (9)
C11	0.4560 (16)	0.1805 (28)	0.1015 (13)
C12	0.4138 (6)	0.2516 (14)	0.1218 (6)
C13	0.3787 (7)	0.1884 (9)	0.1461 (4)
C14	0.4047 (6)	0.1431 (10)	0.1943 (4)
C15	0.3553 (5)	0.0906 (8)	0.1964 (4)
C16	0.3527 (6)	0.0329 (8)	0.2406 (4)
C17	0.3321 (10)	0.1013 (10)	0.2731 (5)
C18	0.4211 (8)	-0.0147 (11)	0.2725 (6)
C19	0.1279 (17)	0.4743 (12)	0.0698 (8)
C20	0.0393 (10)	0.3669 (17)	0.0083 (8)
C21	0.1147 (7)	0.3717 (11)	0.0421 (5)
C22	0.1326 (6)	0.2868 (8)	0.0804 (5)
C23	0.1075 (7)	0.2692 (9)	0.1168 (5)
C24	0.1437 (6)	0.1859 (8)	0.1417 (4)
C25	0.1271 (6)	0.1272 (9)	0.1823 (5)
C26	0.1129 (8)	0.2033 (11)	0.2164 (6)
C27	0.0744 (9)	0.0479 (12)	0.1591 (6)
CS1	0.2913 (12)	0.3550 (12)	0.1914 (6)
CS2	0.1231 (10)	0.4093 (14)	0.3904 (9)
CS3	0.0174 (40)	0.0274 (66)	0.0139 (50)
CL1	0.2794 (4)	0.3649 (4)	0.2452 (2)
CL2	0.3196 (5)	0.4723 (6)	0.1800 (3)
CL3	0.0905 (5)	0.3944 (7)	0.4348 (4)
CL4	0.0800 (4)	0.3263 (5)	0.3409 (2)
CL5	0.3026 (7)	0.0778 (12)	0.0170 (5)
CL6	0.0295 (11)	0.0942 (15)	-0.0246 (9)

dentate anion, e.g., Cl^- , Br^- , OPh^- , SR^-), presumably because of the steric shielding effect of the isopropyl groups in this ligand. These complexes are stable in noncoordinating solvents, but in the presence of Y which is potentially coordinating (such as water, DMF, or THF), the tetrahedral structures are not preserved anymore, and square-pyramidal complexes $\text{Cu}(\text{X})(\text{Y})(\text{HB}(3,5\text{-}i\text{-Pr}_2\text{pz})_3)$ are feasibly formed. Thus, with the present N_3 ligand, the peroxide ion coordinates to the copper ion in a bidentate $\mu\text{-}\eta^2\text{:}\eta^2$ mode, so that the coordination of each copper is square-pyramidal, with a N_3O_2 ligand donor set. Alternatively, if a $\mu\text{-peroxo}$ dicopper complex is prepared with a N_4 ligand, the coordination mode of the peroxide ion is expected to be trans- $\mu\text{-}1,2$, with each copper being five-coordinate with a N_4O donor set. In fact, dioxygen addition to a copper(I) complex with the N_4 ligand, tris[(2-pyridyl)methyl]amine, affords a trans- $\mu\text{-}1,2$ peroxo dinuclear copper(II) complex (**4**) in which the coordination arrangement of each copper ion is described as trigonal-bipyramidal with a N_4O ligand donor set.²⁵

The Cu–Cu separation of **6** is 3.560 (3) Å, which is considerably shorter than that found in a trans- $\mu\text{-}1,2$ dinuclear copper(II) complex (**4**) (4.359 (1) Å)²⁵ but close to the values of oxy-Hc (3.5–3.7 Å)^{41,42} and oxy-Tyr (Å)⁴³ estimated by EXAFS. The other

(35) Sakurai, F.; Suzuki, H.; Moro-oka, Y.; Ikawa, T. *J. Am. Chem. Soc.* **1980**, *102*, 1749–1751.

(36) Kim, K.; Collman, J. P.; Ibers, J. A. *J. Am. Chem. Soc.* **1988**, *110*, 4242–4246.

(37) Bradley, D. C.; Ghotra, J. S.; Hart, F. A.; Hursthouse, M. B.; Raithby, P. R. *J. Chem. Soc., Dalton Trans.* **1977**, 1166–1172.

(38) Haegel, R.; Boeyens, J. C. A. *J. Chem. Soc., Dalton Trans.* **1977**, 648–650.

(39) Kitajima, N.; Fujisawa, K.; Moro-oka, Y. *J. Am. Chem. Soc.* **1990**, *112*, 3210–3212.

(40) Kitajima, N.; Fujisawa, K.; Moro-oka, Y. Manuscript in preparation.

(41) (a) Brown, J. M.; Powers, L.; Kincaid, B.; Larrabee, J. A.; Spiro, T. G. *J. Am. Chem. Soc.* **1980**, *102*, 4210–4216. (b) Woolery, G. L.; Powers, L.; Winkler, M.; Solomon, E. I.; Spiro, T. G. *J. Am. Chem. Soc.* **1984**, *106*, 86–92.

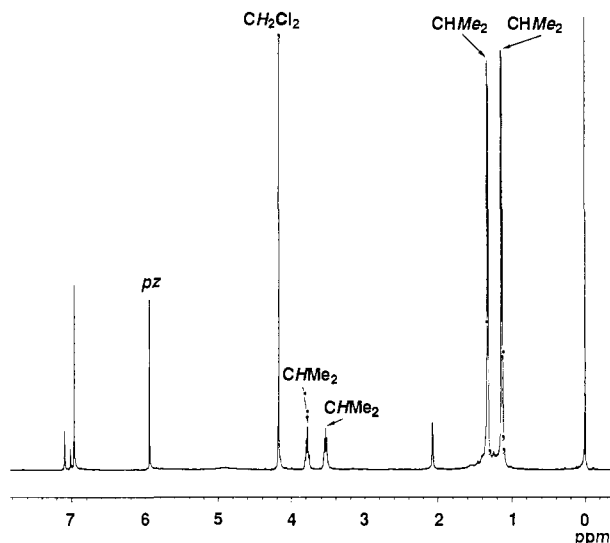


Figure 5. 500 MHz ^1H NMR spectrum of $[\text{Cu}(\text{HB}(3,5\text{-}i\text{-Pr}_2\text{pz})_3)_2(\text{O}_2)]$ (**6**) in toluene- d_8 at $-10\text{ }^\circ\text{C}$.

features of bond distances and angles in **6** are not exceptional.

Formation of μ -Peroxo Complex **7 from **10**.** Although **9** does not form a stable adduct with acetone, with $\text{HB}(3,5\text{-Ph}_2\text{pz})_3$ as a ligand, an acetone adduct **10** is isolable. A solid sample of **10** is reasonably stable even under air, whereas in CH_2Cl_2 the coordinated acetone is dissociated, generating a coordinatively unsaturated species, presumably a monomeric N_3 three-coordinate complex similar to **9**. This is confirmed by ^1H NMR and IR spectra of the solution, which indicate only the existence of free acetone in the solution. Complex **10** does not react with dioxygen in acetone at $-78\text{ }^\circ\text{C}$ but does react readily in CH_2Cl_2 to afford a μ -peroxo dinuclear copper(II) complex (**7**). When the reaction was run at $-78\text{ }^\circ\text{C}$ for 1 h, a purple-colored homogeneous solution was obtained. The O_2 uptake at this stage was 0.5 per mol of **10** determined by manometric measurements, supporting quantitative formation of **7**. Allowing the solution to stand at the same temperature over a period of a few hours, or warming it up to room temperature, causes precipitation of **7** solvated with CH_2Cl_2 . The solid sample $7\cdot 3(\text{CH}_2\text{Cl}_2)$ thus obtained is sparingly soluble in any solvent, but its thermal stability even under air is advantageous in carrying out physicochemical experiments (vide infra).

Magnetism of **6 and **7**.** In Figure 5, the ^1H NMR spectrum of **6** is shown. The spectrum consists of very sharp signals. The chemical shift of the signal assigned to the proton on the pyrazole ring is observed at 5.94 ppm, which is in the chemical shift range (5.7–6.1 ppm) for the pyrazole proton of the copper(I) complexes of $\text{HB}(3,5\text{-}i\text{-Pr}_2\text{pz})_3$,³¹ indicating that **6** is diamagnetic. In fact, the magnetic susceptibility of **6**, determined by the Evans method⁴⁴ at $-10\text{ }^\circ\text{C}$ in toluene, was $0\text{ }\mu\text{B}/\text{mol}$. The thermal stability of **7** in the solid state allowed us to determine the magnetic susceptibility of a solid sample of **7** by the Faraday method, which definitively established the diamagnetism of **7**. These experimental findings provide convincing evidence that a very strong antiferromagnetic interaction ($-2J > 600\text{ cm}^{-1}$) between the two copper(II) ions can be mediated solely by a peroxide ion in the $\mu\text{-}\eta^2\text{:}\eta^2$ coordination mode.

A $\text{trans-}\mu\text{-}1,2$ peroxo dinuclear copper(II) complex (**4**), in which the two copper atoms are bridged solely by the peroxide ion, was reported to be strongly antiferromagnetically coupled.²⁵ Another μ -peroxo dinuclear complex **3** in which the two copper ions are suggested to be bridged solely by a peroxide ion (possibly $\text{cis-}\mu\text{-}1,2$ or $\eta^2\text{:}\eta^2$) was also claimed to be strongly magnetically coupled.²³ The diamagnetic property of oxy-Hc has previously been accepted

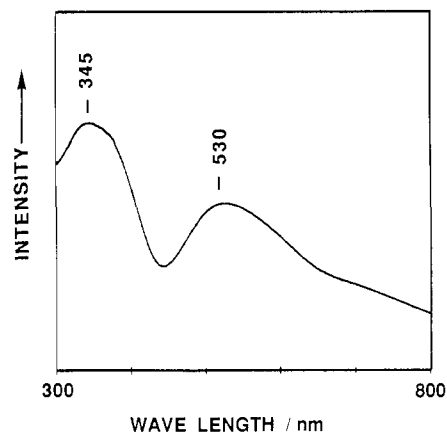


Figure 6. Reflectance spectrum of a solid sample of $[\text{Cu}(\text{HB}(3,5\text{-Ph}_2\text{pz})_3)_2(\text{O}_2)]\cdot 3(\text{CH}_2\text{Cl}_2)$ ($7\cdot 3(\text{CH}_2\text{Cl}_2)$) at room temperature.

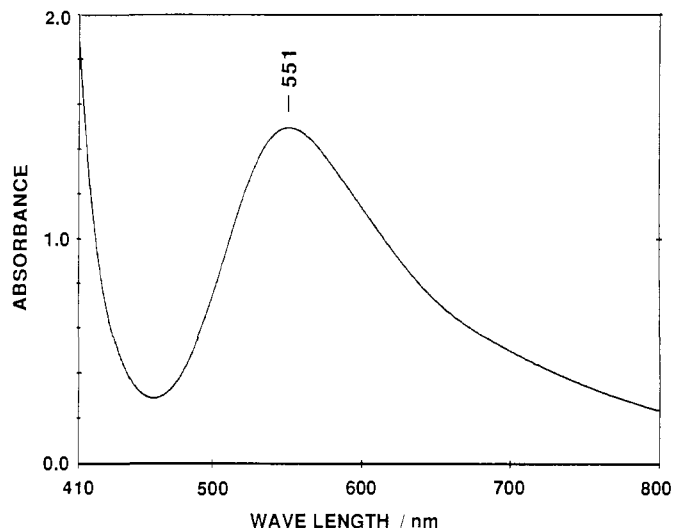


Figure 7. Absorption spectrum of $[\text{Cu}(\text{HB}(3,5\text{-}i\text{-Pr}_2\text{pz})_3)_2(\text{O}_2)]$ (**6**) prepared from **8** in acetone at $-12\text{ }^\circ\text{C}$; **8**, $1.9 \times 10^{-4}\text{ M}$; the cell path length, 1.0 cm.

commonly as a convincing evidence for a dibridged system and the $\text{cis-}\mu\text{-}1,2$ coordination structure of the peroxide ion with an endogenous bridging ligand.¹⁻³ Because it had been believed that the magnetic coupling through the peroxide ion is not very strong, the existence of an endogenous bridging ligand (most likely OH^-) was thought to be responsible for the strong magnetic coupling and resulting in the diamagnetism of oxy-Hc. However, the present experimental results clearly establish that strong antiferromagnetic coupling, even diamagnetism, can be mediated by a peroxide ion alone. Thus, the diamagnetic property of oxy-Hc is not a definitive criterion for the hypothetical $\text{cis-}\mu\text{-}1,2$ coordination structure of the peroxide with an extra bridging ligand.

Absorption Spectra of **6 and **7**.** Both **6** and **7** give rise to the two characteristic absorption bands at ca. 350 and 550 nm with the molar extinction coefficients of ca. $20\,000$ and $1000\text{ cm}^{-1}\text{ M}^{-1}$, respectively. These absorption spectroscopic features are very similar to those of oxy-Hc and oxy-Tyr. The reflectance spectrum of a solid sample of $7\cdot 3(\text{CH}_2\text{Cl}_2)$ (shown in Figure 6) also exhibits two bands whose apparent maxima are consistent with those obtained from the solution sample.

Figure 7 gives the visible absorption spectrum of **6**, which was recorded at $-12\text{ }^\circ\text{C}$ in acetone. This low energy band (551 nm for **6** and 542 nm for **7**) is clearly assignable to $\text{O}_2^{2-} \rightarrow \text{Cu(II)}$ LMCT band, since the molar extinction coefficient is too large for a d-d band; although the tailing shape may be indicative of overlapping of the d-d band at ca. 600–700 nm. On the other hand, assignment of the 350-nm band is not unambiguous at the present stage. Solomon et al. have demonstrated that two characteristic bands of oxy-Hc are ascribed to two distinct O_2^{2-}

(42) Co, M. S.; Hodgson, K. O.; Eccles, T. K.; Lontie, R. *J. Am. Chem. Soc.* **1981**, *103*, 984–986.

(43) Woolery, G. L.; Powers, L.; Winkler, M.; Solomon, E. I.; Lerch, K.; Spiro, T. G. *Biochem. Biophys. Acta* **1984**, *788*, 155–161.

(44) Evans, D. F. *J. Chem. Soc.* **1959**, 2003–2005.

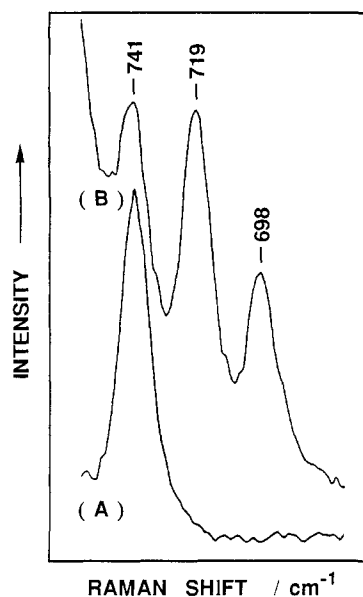


Figure 8. Resonance Raman spectra of $[\text{Cu}(\text{HB}(3,5\text{-}i\text{-Pr}_2\text{pz})_3)_2(\text{O}_2)]$ (**6**) in acetone observed at -40°C : (A) complex **6** prepared with $^{16}\text{O}_2$ and (B) complex **6** prepared with a mixture of $^{16}\text{O}_2\text{-}^{16}\text{O}^{18}\text{O-}^{18}\text{O}_2$ (1:2:1).

\rightarrow Cu(II) LMCT bands: 580 nm, $\pi^*_v(\text{O}_2^{2-}) \rightarrow \text{Cu}(\text{II})$; 350 nm, $\pi^*_o(\text{O}_2^{2-}) \rightarrow \text{Cu}(\text{II})$.^{21,45} This large splitting of the two alternative $\text{O}_2^{2-} \rightarrow \text{Cu}(\text{II})$ charge transitions was originally predicted for the *cis-μ-1,2* peroxide structure, the most generally accepted mode for oxy-Hc. Recently, the MO calculations on the $\mu\text{-}\eta^2\text{:}\eta^2$ structure led to the conclusion that an even larger splitting of $\pi^*_v(\text{O}_2^{2-}) \rightarrow \text{Cu}(\text{II})$ and $\pi^*_o(\text{O}_2^{2-}) \rightarrow \text{Cu}(\text{II})$ LMCT bands is expected for this coordination mode.⁴⁶ In line with this theoretical prediction, it is reasonable to assign the 350-nm band to the $\pi^*_o(\text{O}_2^{2-}) \rightarrow \text{Cu}(\text{II})$ and the 550 nm to $\pi^*_v(\text{O}_2^{2-}) \rightarrow \text{Cu}(\text{II})$ LMCT band. This assignment is in accord with the fact that some copper(II) complexes of $\text{HB}(3,5\text{-}i\text{-Pr}_2\text{pz})_3$ (such as $[\text{Cu}(\text{HB}(3,5\text{-}i\text{-Pr}_2\text{pz})_3)_2(\text{OH})_2]$) do not give a band around 350 nm. However, controversy comes from the contrary observations that a number of other complexes do give rise to a band at ca. 350 nm, although the molar extinction coefficients are not as high as for **6**, e.g.: $\text{Cu}(\text{Cl})(\text{HB}(3,5\text{-}i\text{-Pr}_2\text{pz})_3)$, 362 nm (ϵ , 1950); $\text{Cu}(\text{Br})(\text{HB}(3,5\text{-}i\text{-Pr}_2\text{pz})_3)$, 333 nm (ϵ , 790); $\text{Cu}(\text{OC}_6\text{H}_4\text{-}p\text{-F})(\text{HB}(3,5\text{-}i\text{-Pr}_2\text{pz})_3)$, 344 nm (ϵ , 2700).⁴⁰ This may indicate that the 350-nm band is associated with the pyrazole N \rightarrow Cu(II) LMCT band. Since the molar extinction coefficient of a LMCT band depends strongly on the overlap population between the ligand and metal ion orbitals, the enormous intensities of the 350-nm band observed for **6** and **7** might be ascribed to the unusual coordination structure. Therefore, the possibility that the 350-nm band is due to the pyrazole N \rightarrow Cu(II) LMCT band cannot be excluded completely. Further investigations, including resonance Raman excitation profile experiments, are planned in order to settle the question conclusively.

Resonance Raman Spectra of 6 and 7. Figure 8 shows the Raman spectra of **6** prepared with $^{16}\text{O}_2$ (spectrum A) and a 1:2:1 mixture of $^{16}\text{O}_2/^{16}\text{O}^{18}\text{O}/^{18}\text{O}_2$ (spectrum B) in acetone at -40°C . The spectrum was excited at 514.5 nm in resonance with the LMCT at 551 nm. In the frequency region where the O–O stretching vibration [$\nu(\text{O}–\text{O})$] is expected, a single band was observed at 741 cm^{-1} in spectrum A, but two additional bands were observed at 719 and 698 cm^{-1} in spectrum B. The intensity ratio of the three bands at 741, 719, and 698 cm^{-1} is nearly 1:2:1, as expected from the population ratio of $^{16}\text{O}_2\text{:}^{16}\text{O}^{18}\text{O}\text{:}^{18}\text{O}_2$ in the labeled dioxygen used. The observed isotopic frequency shifts for $^{16}\text{O}^{18}\text{O}$ [$\Delta\nu(^{16}\text{O}^{18}\text{O}) = -22 \text{ cm}^{-1}$] and $^{18}\text{O}_2$ [$\Delta\nu(^{18}\text{O}_2) = -43 \text{ cm}^{-1}$]

are in excellent agreement with the expected shifts for diatomic harmonic oscillators: $\Delta\nu(^{16}\text{O}^{18}\text{O}) = -21$ and $\Delta\nu(^{18}\text{O}_2) = -42 \text{ cm}^{-1}$. Accordingly, the three bands are assigned to $\nu(^{16}\text{O}^{16}\text{O})$, $\nu(^{16}\text{O}^{18}\text{O})$, and $\nu(^{18}\text{O}^{18}\text{O})$ modes, respectively. From this good agreement between the observed and calculated isotopic frequency shifts, we infer that the O–O stretching vibration couples little with other vibrations of the Cu–N₃ moieties. The half-width of the $\nu(^{18}\text{O}_2)$ band is almost the same as those of $\nu(^{16}\text{O}_2)$ and $\nu(^{16}\text{O}^{18}\text{O})$; the width ratio of $\nu(^{16}\text{O}_2)/\nu(^{16}\text{O}^{18}\text{O})/\nu(^{18}\text{O}_2)$ is 1:1.17:1.08. This suggests the presence of only one structure for the binding of $^{16}\text{O}^{18}\text{O}$ to two Cu(II) ions, confirming the symmetric coordination of the peroxide ion. This is consistent with the results for oxy-Hc^{6b} but contrasts with the ones for a μ -peroxy dinuclear complex **1**, which gave a broad Raman band for the $\nu(^{16}\text{O}^{18}\text{O})$ mode and thus suggested asymmetric coordination of the peroxide ion.²¹

The resonance Raman experiment with mixed labeled dioxygen was also accomplished for **7**, supporting the symmetric coordination mode of the peroxide ion in **7** as well as in **6**: $\nu(^{16}\text{O}^{16}\text{O})$, 759 cm^{-1} ; $\nu(^{16}\text{O}^{18}\text{O})$, 744 cm^{-1} ; $\nu(^{18}\text{O}^{18}\text{O})$, 717 cm^{-1} . In order to ascertain the $\mu\text{-}\eta^2\text{:}\eta^2$ structure in the solid state, the Raman spectrum of a solid sample of **7** was explored with 514.5-nm excitation; it exhibited a Raman line ascribed to $\nu(\text{O}–\text{O})$ at 765 cm^{-1} .

A Raman band assignable to the Cu–O stretching vibration of **6** was not identified in the 300–500- cm^{-1} region with excitation at 514.5 nm; this is also the case for oxy-Hc.^{6,7} Since the excitation in the LMCT band appreciably lowers the electron occupation in the peroxide π^* orbital, which is antibonding, the electronic excitation would strengthen and shorten the O–O bond. Then, the change of molecular geometry upon the electronic excitation at LMCT is along the normal coordinate of the $\nu(\text{O}–\text{O})$ mode. Such a mode is expected to gain resonance Raman intensity.⁴⁷ In contrast, the lack of the Cu–O₂ stretching Raman band in the same LMCT excitation implies that the Cu–O₂ distance is little changed in the excited state.

Reaction of 6 and 7 with CO and PPh₃ and Crystal Structure of Carbonyl Copper(I) Complex 11. As reported before, **5** reacts readily with CO and PPh₃, resulting in formation of copper(I) complexes $\text{Cu}(\text{L})(\text{HB}(3,5\text{-Me}_2\text{pz})_3)$ (L = CO and PPh₃) with release of dioxygen.²⁹ In a similar manner, treatment of **6** with CO and PPh₃ gave the corresponding copper(I) complexes **11** and **12**, respectively. Complex **7** also reacts with CO to give a carbonyl complex **13**, whereas it does not react with PPh₃. The inertness of **7** toward PPh₃ is ascribed to its high steric hindrance, since such a phosphine complex cannot be obtained even by the reaction of **10** with PPh₃.

In general, the CO stretching frequency of a carbonyl complex strongly correlates with the electronic properties of the metal center, so that a stronger electron-donating ligand lowers the frequency, because of the π -back bonding interaction effected through the metal center that weakens the CO bond. The stretching frequencies, $\nu(\text{CO})$, of a series of carbonyl complexes with tris(pyrazolyl)borate ligands are as follows: $\text{Cu}(\text{CO})(\text{HB}(3,5\text{-Ph}_2\text{pz})_3)$ (**13**) (2086 cm^{-1}) > $\text{Cu}(\text{CO})(\text{HBpz}_3)$ ⁴⁸ (2083 cm^{-1}) > $\text{Cu}(\text{CO})(\text{HB}(3,5\text{-Me}_2\text{pz})_3)$ ³³ (2066 cm^{-1}) > $\text{Cu}(\text{CO})(\text{HB}(3,5\text{-}i\text{-Pr}_2\text{pz})_3)$ (**11**) (2056 cm^{-1}). This order is consistent with the one expected from the electron-donating property of the ligand. Most carbonyl copper(I) complexes show the CO stretching vibration in the range of 2080–2120 cm^{-1} ,⁴⁹ whereas the CO adduct of Hc^{50,51} exhibits distinctively lower frequencies (2043–2063 cm^{-1}). The CO frequencies of $\text{Cu}(\text{CO})(\text{HB}(3,5\text{-Me}_2\text{pz})_3)$ and

(47) Hirakawa, A. Y.; Tsuboi, M. *Science* **1975**, *188*, 359–361.

(48) Bruce, M. I.; Ostaszewski, A. P. *J. Chem. Soc., Dalton Trans.* **1973**, 2433–2436.

(49) See the following papers and references cited therein: (a) Thompson, J. S.; Whitney, J. F. *Inorg. Chem.* **1984**, *23*, 2813–2819. (b) Sorrell, T. N.; Borovick, A. S. *J. Am. Chem. Soc.* **1987**, *109*, 4255–4260. (c) Patch, M. G.; Choi, H.-K.; Chapman, D. R.; Bau, R.; McKee, V.; Reed, C. A. *Inorg. Chem.* **1990**, *29*, 110–119. (d) Sorrell, T. N.; Vankai, V. A. *Inorg. Chem.* **1990**, *29*, 1687–1692.

(50) Fager, L. Y.; Alben, J. O. *Biochemistry* **1972**, *11*, 4786–4792.

(51) Van der Deen, H.; Hoving, H. *Biophys. Chem.* **1979**, *9*, 169–179.

(45) Eickman, N. C.; Himmelwright, R. S.; Solomon, E. I. *Proc. Natl. Acad. Sci. U.S.A.* **1979**, *76*, 2094–2098.

(46) (a) Ross, P. K.; Solomon, E. I. *J. Am. Chem. Soc.* **1990**, *112*, 5871–5872. (b) Ross, P. K.; Solomon, E. I. *J. Am. Chem. Soc.* **1991**, *113*, 3246–3259.

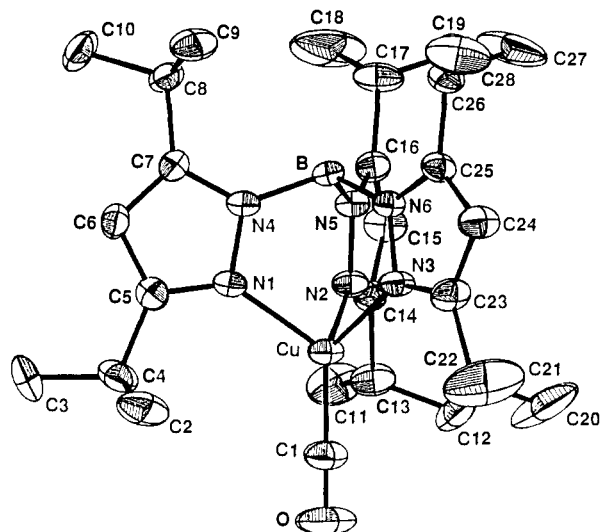


Figure 9. ORTEP view of $\text{Cu}(\text{CO})(\text{HB}(3,5\text{-}i\text{-Pr}_2\text{pz})_3)$ (**11**) (30% probability).

Table IV. Bond Distances (Å) and Angles (deg) for $\text{Cu}(\text{CO})(\text{HB}(3,5\text{-}i\text{-Pr}_2\text{pz})_3)$ (**11**)

Distances			
Cu-C1	1.769 (8)	Cu-N1	2.014 (6)
Cu-N2	2.019 (5)	Cu-N3	2.022 (6)
N1-N4	1.388 (8)	N2-N5	1.375 (8)
N3-N6	1.375 (8)	B-N1	1.541 (11)
B-N2	1.562 (10)	B-N3	1.537 (9)
C1-O	1.118 (10)		
Angles			
N1-Cu-N2	89.8 (2)	N1-Cu-N3	91.6 (3)
N2-Cu-N3	91.1 (2)	C1-Cu-N1	125.1 (4)
C1-Cu-N2	124.7 (3)	C1-Cu-N3	124.2 (3)
Cu-N1-N4	115.4 (5)	Cu-N2-N5	116.7 (4)
Cu-N3-N6	116.1 (4)	N4-B-N5	108.6 (6)
N4-B-N6	110.3 (5)	N5-B-N6	108.2 (6)
B-N4-N1	119.0 (6)	B-N5-N2	117.6 (5)
B-N6-N3	118.7 (6)		

11 are considerably lower than those of conventionally known carbonyl copper(I) complexes. In particular, $\nu(\text{CO})$ of **11** (2056 cm^{-1}) is the lowest among the complexes and very close to the value known for CO adduct of Hc. This may indicate that these ligands can closely mimic the coordination environment of the copper ions in Hc not only geometrically but also electronically, although the ligating atom employed is pyrazole and not histidyl imidazole nitrogen.

In order to ascertain the structural feature which may reflect the unusually low CO stretching vibration frequency, the crystal structure of **11** was determined. Shown in Figure 9 and Table IV are the ORTEP view of **11** and the summary of the bond distances and angles. The ligand arrangement around the copper is distorted tetrahedral. Both C-O and Cu-CO distances are not unusual; the normal distances found for copper(I) carbonyl complexes are the following: C-O, 1.11–1.12 Å; Cu-CO, 1.75–1.78 Å.⁵² The other bond distances and angles are also not exceptional.

Molecular Orbital Analysis. In order to identify electronic factors responsible for the unusual $\mu\text{-}\eta^2\text{-}\eta^2$ peroxide coordination in **5–7** and the experimentally observed diamagnetism, we have performed extended Hückel MO calculations of a simplified model, $[(\text{NH}_3)_3\text{Cu}]_2(\text{O}_2)^{2+}$. This theoretical section includes also an analysis for $[(\text{NH}_3)_4\text{Cu}]_2(\text{O}_2)^{2+}$, modeling **4**, to probe the elec-

tronic origin that differentiates its geometrical features from those of $[(\text{NH}_3)_3\text{Cu}]_2(\text{O}_2)^{2+}$.

Given $\mu\text{-}\eta^2\text{-}\eta^2$ O_2 between two Cu atoms, the square-pyramidal N_3O_2 arrangement that **6** possesses at each Cu was initially addressed by calculating the total energy of $[(\text{NH}_3)_3\text{Cu}]_2(\text{O}_2)^{2+}$ as a function of three angles (α , β , ϕ). This is shown in Figure 10, where a convenient starting structure consists of a planar $\text{N}_2\text{-Cu}(\text{O}_2)\text{CuN}_2$ frame to which two axial NH_3 groups coordinate from the same side of the plane. In the middle of Figure 10 is shown a potential energy curve for the rocking motion (α) of the two $\text{Cu}(\text{NH}_3)_3$ units, where the $\text{Cu-N}_{\text{basal}}$ and $\text{Cu-N}_{\text{apical}}$ distances are set as 1.95 and 2.26 Å, respectively. Also the Cu-O (1.91 Å) and O-O (1.41 Å) distances are fixed. The calculations revealed a minimum at $\alpha = 15^\circ$ that approximately corresponds to the N2-Cu-O₂ angle of 25° or the dihedral angle of 22° between the N1N2Cu and CuOO planes in **6**.

One $\text{Cu}(\text{NH}_3)_3$ unit is then rotated (ϕ) along the Cu-Cu axis (on Figure 10, right), with the angle α being fixed at 15° . While the rotation has a barrier of 0.4 eV, stability of the two limiting conformers, cis ($\phi = 0^\circ$) and trans ($\phi = 180^\circ$) with respect to the "apical" NH_3 groups, is shown to be nearly the same. Only the very small energy difference of 0.001 eV prefers the trans conformer which is analogous to the geometry of **6**. We have also examined puckering (β) of the CuO_2Cu skeleton for the cis conformer with $\alpha = 15^\circ$. As the potential curve on the left of Figure 10 shows, the molecule is gradually destabilized toward higher β , and it is evident that the planar CuO_2Cu geometry is favored electronically. A similar uphill energy curve was obtained when the trans conformer ($\alpha = 15^\circ$, $\phi = 180^\circ$) was puckered. On the whole, our calculations on the model, $[(\text{NH}_3)_3\text{Cu}]_2(\text{O}_2)^{2+}$, reproduce reasonably the main geometrical features of **6**.

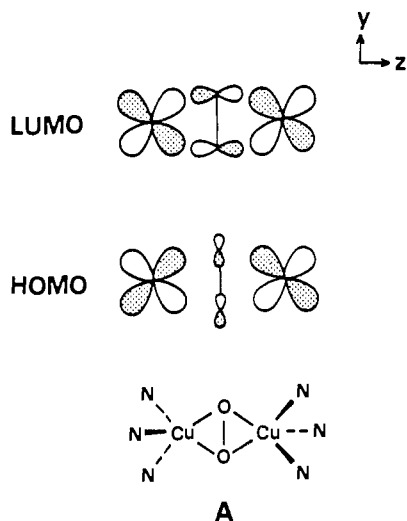
In Figure 11, the molecular orbitals for $[(\text{NH}_3)_3\text{Cu}]_2(\text{O}_2)^{2+}$ ($\alpha = 15^\circ$, $\beta = 0^\circ$, $\phi = 180^\circ$) are constructed by allowing two $(\text{NH}_3)_3\text{Cu}^{2+}$ fragments and O_2^{2-} to interact. Each $(\text{NH}_3)_3\text{Cu}^{2+}$ fragment carries five frontier orbitals primarily made up of Cu 3d orbitals which split in a three-below-two pattern. For the d^9 Cu^{2+} configuration, the singly-occupied level (SOMO) is of the Cu yz type with a slight admixture of xz . In the absence of the bridging O_2^{2-} unit, the direct through-space interaction of the $(\text{NH}_3)_3\text{Cu}^{2+}$ orbitals is small, so that two such fragments give simply in- and out-of-phase pairs of each fragment orbital. Not shown in Figure 11 is a pair of unoccupied Cu spd hybrids pointing toward each other, which lie at $-8 \sim -9$ eV in energy. The out-of-phase combination of the spd hybrids takes part in stabilization of the $\text{O}_2 \pi^*_{\sigma}$, and π^*_{σ} orbitals overlap with Cu-Cu $1b_u$ and $1b_g$ in the lower d-block. These fragment orbitals, however, are all occupied, and their interactions do not contribute to Cu-O₂-Cu bonding.

The most important aspect of Figure 11 is destabilization of the out-of-phase combination of $(\text{NH}_3)_3\text{Cu}$ SOMO, designated $2b_g$, through interaction with $\text{O}_2 \pi^*_{\sigma}$, while its in-phase counterpart, $2a_u$, remains nearly untouched. The consequence is the sizable HOMO-LUMO gap of 0.883 eV for $[(\text{NH}_3)_3\text{Cu}]_2(\text{O}_2)^{2+}$, which should account for the observed diamagnetism of **6**. Top views of these orbitals are depicted below in A. The strong antibonding nature between Cu yz and $\text{O}_2 \pi^*_{\sigma}$ is evident in the LUMO.

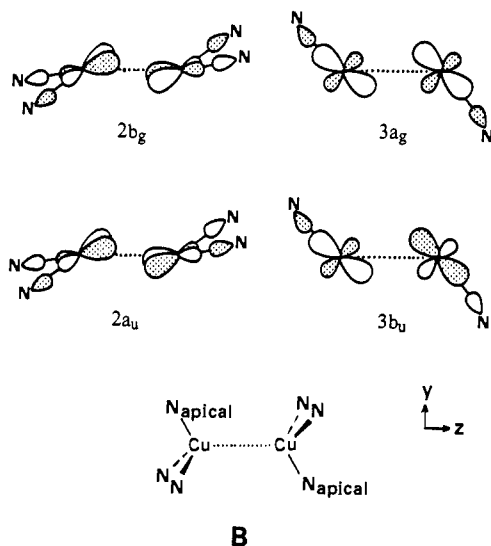
Recently, spin-unrestricted SCF-X α SW calculations on $[(\text{NH}_3)_2\text{Cu}]_2(\text{O}_2)^{2+}$ have been reported.⁴⁶ Although the model Cu fragment differs from ours, its HOMO and LUMO have orbital shapes very similar to those shown in A. A large HOMO-LUMO gap was also noticed which gave rise to an $-2J$ value as great as 5660 cm^{-1} .

We comment here on the Cu-N bonds in **6**. In the X-ray structure of **4**, the "apical" Cu-N bonds are substantially longer than the "basal" Cu-N bonds. To ascertain if there is an electronic reason behind such a trend, we have recalculated on $[(\text{NH}_3)_3\text{Cu}]_2(\text{O}_2)^{2+}$ ($\alpha = 15^\circ$, $\beta = 0^\circ$, $\phi = 180^\circ$) where all the Cu-N distances are set equal at 1.95 Å. Then comparison of the Cu-N overlap population (P) showed that coordination of the "basal" NH_3 groups was clearly stronger than the "apical" NH_3 , $P(\text{Cu-N}_{\text{apical}}) = 0.299$ vs $P(\text{Cu-N}_{\text{basal}}) = 0.349$, in accord with

(52) See the following papers and the references cited therein: (a) Churchill, M. R.; DeBoer, B. G.; Rotella, F. J.; Abu Salah, O. M.; Bruce, M. I. *Inorg. Chem.* **1975**, *14*, 2051–2056. (b) Gagne, R. R.; Allison, J. L.; Gall, R. S.; Koval, C. A. *J. Am. Chem. Soc.* **1977**, *99*, 7170–7178. (c) Doyle, G.; Eriksen, K. A.; Van Engen, D. *Inorg. Chem.* **1983**, *22*, 2892–2895.

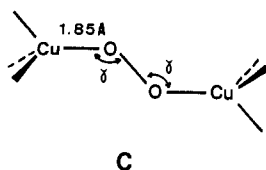


the experimental observation. The different Cu-N bond strength can be traced to the four higher lying frontier orbitals of $[(\text{NH}_3)_3\text{Cu}]^{2+}$ in Figure 11. Although these frontier orbitals are mainly made of Cu d's, NH_3 lone pair orbitals are admixed in an antibonding manner. This is why these levels are high in energy. As schematically shown in B, the upper two levels, $2b_g$



and $2a_u$, have a contribution from the basal NH_3 lone pairs, while the lower two levels, $3a_g$ and $3b_u$, contain the apical NH_3 lone pairs. For the CuO_2Cu (d^9-d^9) system, the $2b_g$ orbital becomes unoccupied resulting in diminution of the $\text{Cu}-\text{N}_{\text{basal}}$ antibonding character. This is the primal cause for the stronger $\text{Cu}-\text{N}_{\text{basal}}$ bond relative to $\text{Cu}-\text{N}_{\text{apical}}$ bond. Conversely, we may state that observation of the long $\text{Cu}-\text{N}_{\text{apical}}$ bond is evidence for the $2b_g$ HOMO. By the same reason, the apical nitrogen was computed to be more negatively charged (-0.393 e) than the basal nitrogen (-0.232 e).

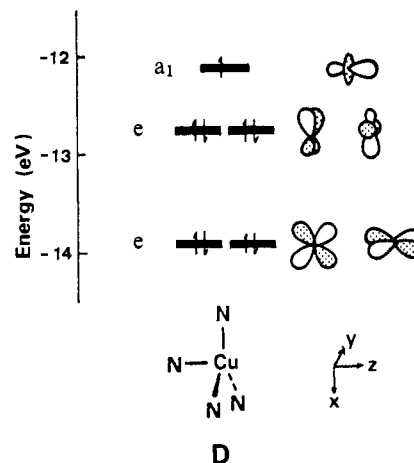
Turning to an alternative O_2 coordination mode, we have roughly optimized the $\mu\text{-}\eta^1\text{:}\eta^1$ O_2 geometry of $[(\text{NH}_3)_3\text{Cu}]_2(\text{O}_2)^{2+}$ by varying the Cu-O-O angle from 90° to 180° as shown in C.



The energy curve obtained therefrom, assuming a singlet ground state, was flat, and a shallow minimum appeared at $\gamma = 130^\circ$ where the Cu-O overlap population was also maximal. This $\mu\text{-}\eta^1\text{:}\eta^1$ O_2 structure ($\gamma = 130^\circ$) of $[(\text{NH}_3)_3\text{Cu}]_2\text{O}_2^{2+}$ is 0.267 eV

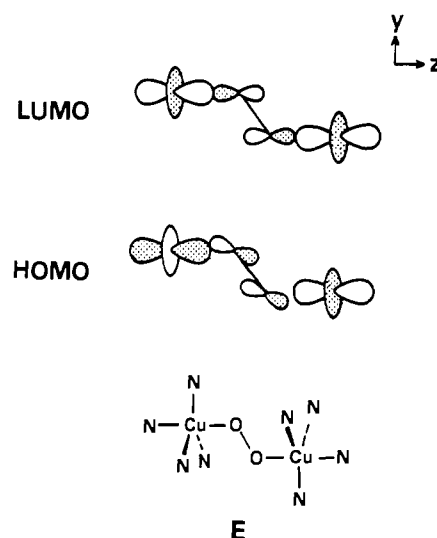
less stable than the $\mu\text{-}\eta^2\text{:}\eta^2$ O_2 structure ($\alpha = 15^\circ$, $\beta = 0^\circ$, $\gamma = 180^\circ$). Thus, the observed geometrical preference of **6** gains a theoretical support. Interestingly, on going from $\mu\text{-}\eta^2\text{:}\eta^2$ O_2 to $\mu\text{-}\eta^1\text{:}\eta^1$ O_2 , the HOMO-LUMO gap drops substantially from 0.883 to 0.089 eV, because the Cu $yz\text{-O}_2$ $\pi^*\sigma$ antibonding character in the $\mu\text{-}\eta^1\text{:}\eta^1$ O_2 LUMO is weaker. We believe that $\mu\text{-}\eta^1\text{:}\eta^1$ O_2 complexes of a type $(\text{L}_3\text{Cu})_2\text{O}_2^{2+}$ (L, neutral σ -donor ligand), if made, should be paramagnetic, or that its antiferromagnetic coupling should be very weak.

Now consider the electronic structure of $[(\text{NH}_3)_4\text{Cu}]_2(\text{O}_2)^{2+}$ as a model for **4**. The C_{3v} $(\text{NH}_3)_4\text{Cu}^{2+}$ fragment has five frontier orbitals primarily made of Cu d orbitals (see D), as is the case of $(\text{NH}_3)_3\text{Cu}^{2+}$. An important facet of their splitting pattern is



that the highest level (SOMO) consists of Cu z^2 (a_1) and that the Cu yz orbital is in the lowest e set. This contrasts to the high-lying Cu yz of $(\text{NH}_3)_3\text{Cu}^{2+}$. The low positioning of Cu yz is the main reason that the complex **4** prefers a $\mu\text{-}\eta^1\text{:}\eta^1$ O_2 geometry. For $[(\text{NH}_3)_4\text{Cu}]_2(\mu\text{-}\eta^2\text{:}\eta^2$ $\text{O}_2)^{2+}$, the Cu $yz\text{-O}_2$ $\pi^*\sigma\text{-Cu}$ yz antibonding molecular orbital, which is analogous to the LUMO of $[(\text{NH}_3)_3\text{Cu}]_2(\mu\text{-}\eta^2\text{:}\eta^2$ $\text{O}_2)^{2+}$, is forced to be occupied, and such an O_2 coordination mode becomes unfeasible. In fact, our calculations on $[(\text{NH}_3)_4\text{Cu}]_2(\mu\text{-}\eta^2\text{:}\eta^2$ $\text{O}_2)^{2+}$ put the $\mu\text{-}\eta^2\text{:}\eta^2$ O_2 geometry 4.56 eV higher in energy than $\mu\text{-}\eta^1\text{:}\eta^1$ O_2 ($\gamma = 107.0^\circ$).

Bonding properties of $\mu\text{-}\eta^1\text{:}\eta^1$ M-O-O-M skeletons have been discussed earlier by one of us.⁵³ Suffice it here to show the HOMO and LUMO of $[(\text{NH}_3)_4\text{Cu}]_2(\mu\text{-}\eta^1\text{:}\eta^1$ $\text{O}_2)^{2+}$ in E. These



levels are reminiscent of the a_1 SOMO of $\text{Cu}(\text{NH}_3)_4$, consisting of in- and out-of-phase combinations of Cu z^2 into which O_2 orbitals are mixed. The O_2 components are complicated hybrids

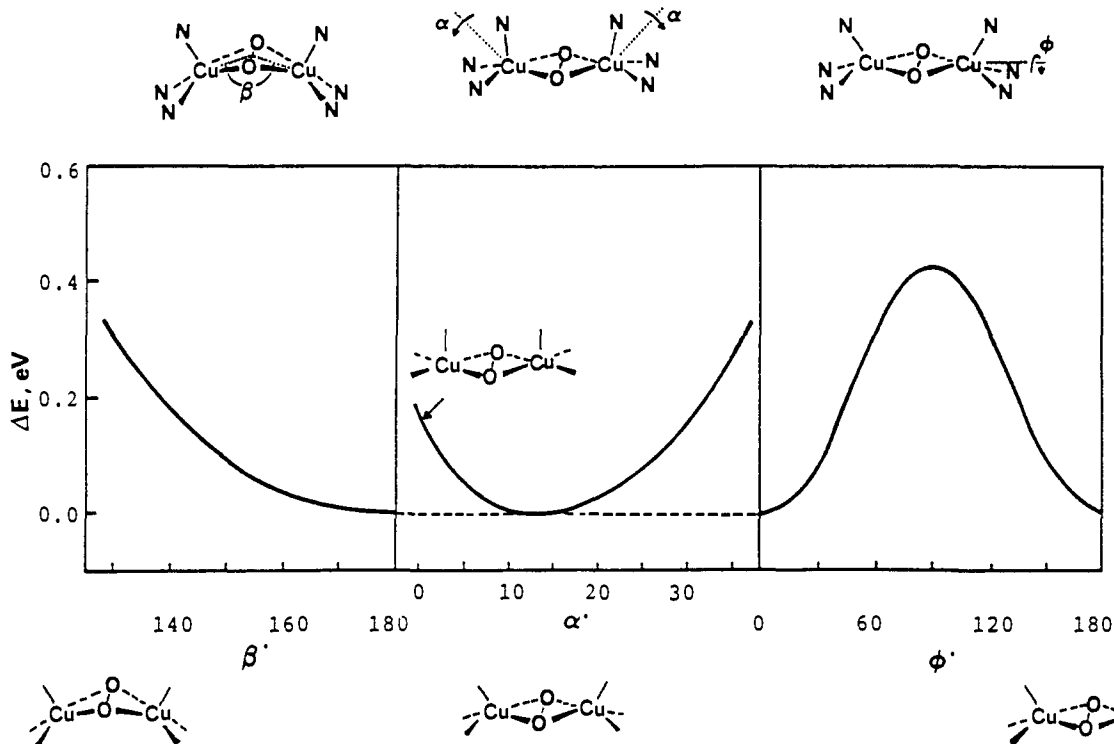


Figure 10. Potential energy curves for deformation of $[(\text{NH}_3)_3\text{Cu}]_2(\mu\text{-}\eta^2\text{:}\eta^2\text{O}_2)^{2+}$. The variables is either α , β , or ϕ defined above each curve.

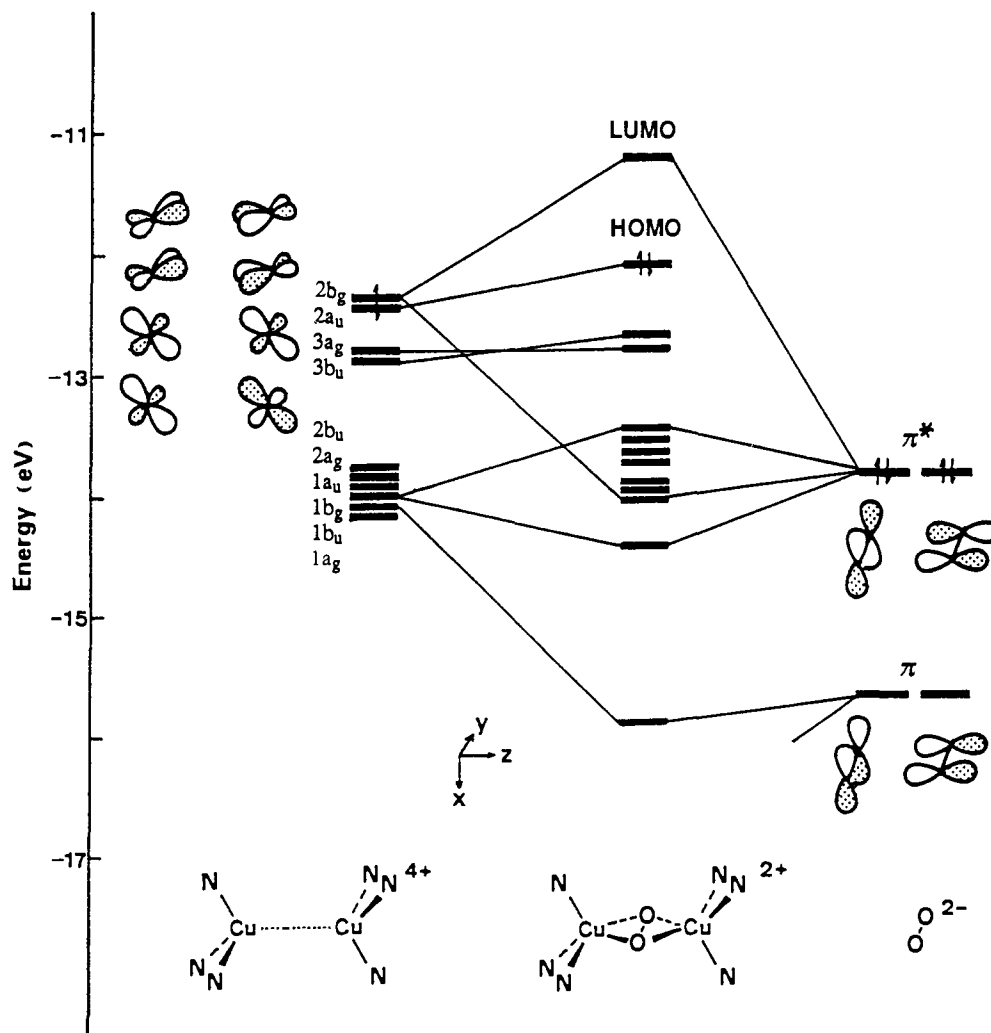
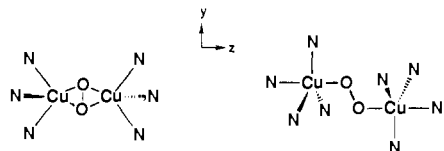


Figure 11. Interaction diagram for the frontier orbitals of $[(\text{NH}_3)_3\text{Cu}]_2(\mu\text{-}\eta^2\text{:}\eta^2\text{O}_2)^{2+}$ ($\alpha = 15^\circ$, $\beta = 0^\circ$, $\phi = 180^\circ$). At right two $(\text{NH}_3)_3\text{Cu}^{2+}$ fragments are combined and held a staggered (D_{3h}) geometry. Then the $[(\text{NH}_3)_3\text{Cu}]^{4+}$ composite is mixed with O_2^{2-} .

Table V. Charges and Overlap Populations for $[(\text{NH}_3)_3\text{Cu}]_2\mu\text{-}\eta^2\text{-}\eta^2\text{O}_2^{2+}$ and $[(\text{NH}_3)_4\text{Cu}]_2(\mu\text{-}\eta^1\text{-}\eta^1\text{O}_2)^{2+}$


P(Cu-N _{apical})	0.299	P(Cu-N _{axial})	0.313
P(Cu-N _{basal})	0.349	P(Cu-N _{equatorial})	0.319
P(Cu-O ₂) ^{a)}	0.357		0.224
P(O-O)	0.381		0.394
Q(Cu)	+0.498		+0.232
Q(O ₂)	-1.075		-1.439

^aThe sum of two Cu-O overlap populations.

of π^b , π^* , and σ^* , σ , and the different strength of the Cu-O₂ antibonding interaction provides the HOMO-LUMO separation of 0.275 eV. The energy gap is evidently smaller than that of $[(\text{NH}_3)_3\text{Cu}]_2(\mu\text{-}\eta^2\text{-}\eta^2\text{O}_2)^{2+}$ but is larger compared with the hypothetical $[(\text{NH}_3)_3\text{Cu}]_2(\mu\text{-}\eta^1\text{-}\eta^1\text{O}_2)^{2+}$. From this value alone, it is difficult to conclude whether $[(\text{NH}_3)_4\text{Cu}]_2(\mu\text{-}\eta^1\text{-}\eta^1\text{O}_2)^{2+}$, and thus **4**, is diamagnetic or paramagnetic. If the Coulomb term, $J_{aa}-J_{ab}$, is assumed to be 5 eV,⁵⁴ the size of antiferromagnetic coupling ($2J$) would be ca. -120 cm^{-1} . Experimentally, on the other hand, the complex **4** has been claimed to be diamagnetic based on its sharp ¹H NMR signals as well as the lack of EPR signals.²⁵

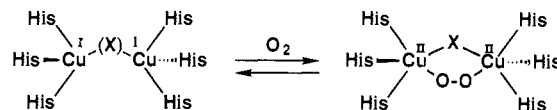
Finally Table V compares overlap populations (P) and charges (Q) calculated for $[(\text{NH}_3)_3\text{Cu}]_2(\mu\text{-}\eta^2\text{-}\eta^2\text{O}_2)^{2+}$ and $[(\text{NH}_3)_4\text{Cu}]_2(\mu\text{-}\eta^1\text{-}\eta^1\text{O}_2)^{2+}$. We have mentioned earlier that P(Cu-N_{apical}) of the former complex is much smaller than P(Cu-N_{basal}). In the case of the latter complex, no significant difference in size was observed between P(Cu-N_{axial}) and P(Cu-N_{equatorial}), while P(Cu-N_{axial}) was very slightly smaller, both of which lay in between the values of P(Cu-N_{apical}) and P(Cu-N_{basal}) for $[(\text{NH}_3)_3\text{Cu}]_2(\text{O}_2)^{2+}$. These trends closely correlate with the experimentally determined Cu-N bond lengths of **4** and **6**: Cu-N_{axial} = 2.104 (6) Å and Cu-N_{equatorial}(av) = 2.07 (1) Å vs Cu-N_{apical} = 2.258 (8) Å and Cu-N_{basal}(av) = 2.00 (1) Å. As for the Cu-O₂ interactions, $[(\text{NH}_3)_3\text{Cu}]_2\text{O}_2^{2+}$ gives a greater overlap population, indicating tighter Cu-($\mu\text{-}\eta^2\text{-}\eta^2\text{O}_2$)-Cu bonding. The result may have relevance to the irreversible O₂ coordination for **6** and to the contrasting reversible O₂ binding for **4**. On the other hand, P(O-O) does not differ much between the two model complexes. It should be noted here that the O p_x orbitals do not contribute either to P(Cu-O) or P(O-O). Thus the Cu-O₂-Cu bonds are formed through interactions in the yz molecular plane. As the number of N-donor ligands increases, from $[(\text{NH}_3)_3\text{Cu}]_2(\text{O}_2)^{2+}$ to $[(\text{NH}_3)_4\text{Cu}]_2(\text{O}_2)^{2+}$, more electrons drift into the Cu-O₂-Cu portion, leading to a smaller positive charge (Q) on Cu. At the same time, the negative charge on O₂ increases.

Biological Relevance: Possibility of the $\mu\text{-}\eta^2\text{-}\eta^2$ Peroxide Coordination in Oxy-Hc and Oxy-Tyr. The physicochemical properties of **6** and **7** as well as **5** are summarized in Table VI and compared with those known for oxy-Hc and oxy-Tyr. The remarkable similarities in many respects between these $\mu\text{-}\eta^2\text{-}\eta^2$ peroxo dinuclear complexes and oxy-Hc and oxy-Tyr are evident, including (1) diamagnetism, (2) characteristic absorption bands, (3) low O-O stretching vibration frequency, (4) symmetric coordination mode of the peroxide, (5) Cu-Cu separation, and (6) absence of the Cu-O band in resonance Raman spectrum in the excitation of O₂²⁻ → Cu(II) LMCT band around 550 nm. In addition, the $\nu(\text{CO})$ for copper(I) carbonyl complexes corresponding to **5** and **6** are close to that of CO adduct of Hc. The spectroscopic characterizations of **5-7** have been accomplished with solution samples, and there may be some debate whether these properties are associated with the $\mu\text{-}\eta^2\text{-}\eta^2$ peroxide structure which was established by X-ray crystallography for a solid structure. The serious question which one may argue is that the $\mu\text{-}\eta^2\text{-}\eta^2$

structure is deformed in solution and results in rearrangement to a $\mu\text{-}\eta^1\text{-}\eta^1$ structure. However, this possibility can be excluded, since as we mentioned already, the extended Hückel MO calculations led us to predict reasonably that if such a peroxide complex was formed, it should be paramagnetic or weakly antiferromagnetic. Furthermore, all data obtained with the solid sample including the O-O stretching vibration frequency, reflectance spectrum, and magnetic susceptibility are identical to those observed for solution samples, supporting our conclusion that the $\mu\text{-}\eta^2\text{-}\eta^2$ structure is preserved in solution. We thus believe that all characteristic properties summarized in Table VI are associated with the N₃Cu($\mu\text{-}\eta^2\text{-}\eta^2\text{-O}_2^{2-}$)CuN₃ chromophore. In order to ascertain this point more clearly, further investigations including EXAFS and absorption spectroscopy on the solid sample are now in progress.

Despite extensive efforts, no synthetic example which can mimic the physicochemical characteristics of oxy-Hc and oxy-Tyr as closely as **5-7** has been known to date,^{15,16} although mimicking of the magnetism and absorption spectrum was accomplished to some extent. From this we infer that the Cu(O₂)Cu chromophore in oxy-Hc or oxy-Tyr is structurally, and consequently spectroscopically, very unique. Therefore, the close resemblance experimentally observed between the $\mu\text{-}\eta^2\text{-}\eta^2$ peroxo complexes and oxy-Hc and oxy-Tyr raises a new possibility that these proteins also possess the particular coordination mode of the peroxide ion, $\mu\text{-}\eta^2\text{-}\eta^2$. The possibility of $\mu\text{-}\eta^2\text{-}\eta^2$ coordination of the peroxide was hypothesized previously,⁶ as one of the plausible models for oxy-Hc. However, this structural mode has not been considered seriously, because such a synthetic example, of which the structure was established by X-ray crystallography, was unknown prior to the present work. Recently, the possibility was discussed by Blackburn and Karlin based on the EXAFS study on complexes **3**, but still there was a debate whether the complexes might have another structure such as cis- $\mu\text{-}1,2$.²⁴

The coordination structure of dioxygen in oxy-Hc has been the subject of extensive physicochemical studies for quite some time. An X-ray analysis^{4,5} of deoxy-Hc and EXAFS works^{41,42} on oxy-Hc indicated a Cu-Cu separation of ca. 3.6 Å. Loehr et al. elucidated that the dioxygen binds to the dinuclear copper site as a peroxide ion with a symmetric coordination mode, based on the resonance Raman study using mixed labeled dioxygen.^{6b} This result also suggested that the two copper(I) ions in deoxy-Hc should be oxidized to copper(II) ions in oxy-Hc. The oxidation to copper(II) ions in oxy-Hc was further supported by XPS and XANES spectroscopy.^{9,10,41} Accordingly, the diamagnetism of oxy-Hc is ascribed to the strong magnetic coupling between the two copper(II) ions, and because of this striking characteristic, the most likely binding fashion of dioxygen at the dicopper site in Hc has been generally accepted as follows. The dicopper site,



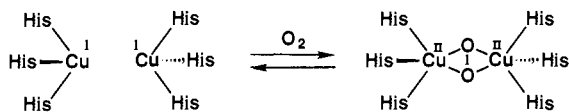
at least in oxy-Hc, is suggested to be bridged with an endogenous ligand (X) which is responsible for the strong magnetic coupling. The peroxide coordination is, thereby, ascribed to cis- $\mu\text{-}1,2$. As the most likely bridging ligand, a protein residue such as tyrosine phenoxide or serine alkoxide was previously proposed. However, the X-ray crystallographic data for deoxy-Hc^{4,5} excluded this possibility, and thus hydroxide ion was recently accepted as the most likely candidate.^{55,56} This hypothesis, however, has not been proven experimentally yet. No spectroscopic evidence for the existence of such a bridging ligand has ever been provided. Rather, the X-ray analysis of deoxy-Hc did not show any electron density between the two copper atoms which could be attributable to a hydroxide ligand, although the resolution is not high enough to address this point definitively.^{5b}

The new model for dioxygen binding in Hc we propose here is a simple dioxygen addition to the dicopper site, resulting in the

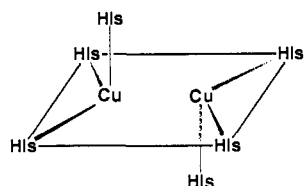
(54) Hay, P. J.; Thibeault, J. C.; Hoffmann, R. *J. Am. Chem. Soc.* **1975**, *97*, 4884-4899.

(55) Loehr, T. M.; Shiemke, A. K. *Biological Applications of Raman Spectroscopy*; Spiro, T. G., Ed.; Wiley: New York, 1988; Vol. IV.
(56) Loroesch, J.; Haase, W. *Biochemistry* **1986**, *25*, 5850-5857.

$\mu\text{-}\eta^2\text{:}\eta^2$ coordination of the peroxide. With this model, we do not need to assume the existence of an endogenous bridging ligand,



because we now know experimentally and theoretically that the $\mu\text{-}\eta^2\text{:}\eta^2$ peroxide alone can mediate a very strong magnetic interaction between the two copper(II) ions, accounting for the diamagnetism. Furthermore, structural comparison of the $\text{N}_3\text{-Cu}(\text{O}_2)\text{CuN}_3$ moiety in **6** and the X-ray structure^{5c} of deoxy-Hc supports the proposal favorably. Each copper ion in deoxy-Hc is supported by three imidazole nitrogen atoms from the protein chains, with the Cu–Cu separation of 3.54 Å. The coordination structures of the two copper ions are close to each other, consisting of two short Cu–N bonds and the other distinctly longer Cu–N bond. The four nitrogen ligands of short Cu–N bond (Cu–N, 1.95–2.10 Å), together with the two copper ions, comprise a planar $\text{N}_2\text{Cu-CuN}_2$ frame, to which the apical two nitrogen atoms (with elongated Cu–N lengths (2.66 and 2.77 Å)) coordinate from opposite sides of the plane. Thus, the configuration of the apical ligands is trans and not cis. All these structural features of the coordination structure of the dicopper site in deoxy-Hc are very similar to the $\text{N}_3\text{Cu}(\text{O}_2)\text{CuN}_3$ moiety in **6** (see Figure 4), except the shorter Cu–N_{apical} distance of 2.26 Å. Accordingly, one can imagine easily that a peroxide ion would fit in the planar $\text{N}_2\text{-Cu-CuN}_2$ frame in deoxy-Hc without a serious structural change in the $\mu\text{-}\eta^2\text{:}\eta^2$ mode.



Schematic view of the dicopper site in deoxy-Hc

The solid basis supporting the existence of the endogenous bridging ligand, and thus the cis- $\mu\text{-}1,2$ coordination mode of the peroxide in oxy-Hc, lies on the extensive spectroscopic studies on met-Hc.^{57,58} The existence of a bridging ligand mediating the strong magnetic coupling is evident in met-Hc because of their antiferromagnetic properties. In particular, met-azide-Hc, which is obtained by azide treatment of oxy-Hc, has been studied in detail and it almost certainly has a $\mu\text{-hydroxo, } \mu\text{-}1,3$ azido structure.^{59,60} However, one should keep in mind that these met-Hc are products of some chemical reactions of Hc, so that the dicopper site in met-Hc may be reconstructed to involve the extra bridging ligand, which is not endogenous but exogenous, such as OH⁻ originating from water. In fact, a preliminary experiment of ours showed that treatment of **6** with azide ion resulted in the conversion of **6** to a $\mu\text{-hydroxy, } \mu\text{-}1,3$ azide dinuclear copper(II) complex, which serves as an accurate synthetic model for met-azide-Hc.⁶¹

The other aspect of oxy-Hc which has been argued extensively is the origin of the two characteristic absorption bands observed at ca. 350 and 580 nm. There is a consensus for the assignment of the 580-nm band to the $\text{O}_2^{2-} \rightarrow \text{Cu}(\text{II})$ LMCT band. However, the assignment of the 350-nm band was not firmly established

yet. Initial resonance Raman work on oxy-Hc suggested that this band was ascribed to the histidyl imidazole N $\rightarrow \text{Cu}(\text{II})$ LMCT band.^{6,62} Conversely, the Raman excitation profile of the 350-nm band was interpreted in terms of its assignment to a $\text{O}_2^{2-} \rightarrow \text{Cu}(\text{II})$ LMCT.⁷ Furthermore, based on the spectroscopic work on met-azide-Hc and its model complexes,^{59,60} together with theoretical calculations, Solomon et al. claimed that the band is attributable to $\pi^*(\text{O}_2^{2-}) \rightarrow \text{Cu}(\text{II})$ LMCT band. Now, it is experimentally established that the $\mu\text{-}\eta^2\text{:}\eta^2$ peroxo complexes **5–7** in solution give the absorption spectra consisting of two characteristic bands which are very similar to oxy-Hc not only qualitatively but also quantitatively. The band at ca. 550 nm is definitely ascribed to a $\text{O}_2^{2-} \rightarrow \text{Cu}(\text{II})$ LMCT band as for oxy-Hc. However, we refrain here a conclusive explanation for the origin of the 350-nm band; possible assignments are (1) $\pi^*(\text{O}_2^{2-}) \rightarrow \text{Cu}(\text{II})$ LMCT, (2) pyrazole N $\rightarrow \text{Cu}(\text{II})$ LMCT, and (3) overlapping of both LMCT bands. Thus, there is a possibility that the character of the band of **5–7** might be different from that observed for oxy-Hc. But still, we comment here that the close resemblance of the electronic spectra of **5–7** and oxy-Hc (or oxy-Tyr) does support our proposal that oxy-Hc also possesses $\mu\text{-}\eta^2\text{:}\eta^2$ peroxide structure.

Several $\mu\text{-peroxo}$ dicopper complexes, including **3**, were reported to be prepared by low-temperature dioxygen treatments of dicopper(I) complexes in which each copper ion is coordinated with three nitrogen atoms. Although the dioxygen adducts were not fully characterized, it is most likely that the formed adducts possess the $\mu\text{-}\eta^2\text{:}\eta^2$ structure, since no bridging ligand other than dioxygen is available in these systems. Here, it is notable that all these species give two strong absorption bands at ca. 350 and 450–550 nm, respectively: **3** ($n = 3$)²³ 365 (15 000), 600 (1200) nm; **3** ($n = 4$)⁶³ 360 (15 000), 458 (5000) nm; **3** ($n = 5$)⁶³ 360 (21 400), 520 (1200) nm; $[\text{Cu}_2(\text{XYL-F})(\text{O}_2)]^{+64}$ 360 (18 700), 515 (1300) nm; $[\text{Cu}_2(\text{tpmc})(\text{O}_2)]^{2+65}$ 472 (2900) nm; $[\text{Cu}_2(\text{DF}_2\text{DIEN}_2)(\text{O}_2)]^{2+66}$ 360 (–), 550 (1060) nm; $[\text{Cu}[\text{Bz}(\text{NMI})_2\text{N}_3]]_2(\text{O}_2)^{2+67}$ 360 (–), 550 (–) nm. These results may indicate that the 350-nm band is associated with the $\text{N}_3\text{Cu}[\mu\text{-}\eta^2\text{:}\eta^2\text{O}_2^{2-}]\text{CuN}_3$ chromophore, which causes us to favor the assignment of the 350-nm band observed for **5–7** to a $\text{O}_2^{2-} \rightarrow \text{Cu}(\text{II})$ LMCT band.

Finally, it should be noted that both oxy-Hc and the $\mu\text{-}\eta^2\text{:}\eta^2$ peroxo complexes give very low O–O stretching frequencies. The typical $\nu(\text{O-O})$ known for transition-metal-peroxo complexes are 800–900 cm^{-1} ,⁶⁸ and the lowest one known to date is 803 cm^{-1} reported for the peroxo copper complex **1**. Although this aspect has not been given much attention in the previous structural arguments on oxy-Hc, we believe that the very low O–O stretching frequency reflects the unusual side-on $\mu\text{-}\eta^2\text{:}\eta^2$ structure of the peroxide ion. The MO calculations on $\mu\text{-}\eta^2\text{:}\eta^2$ peroxo dicopper(II) complex suggested a significant contribution of a back-bonding interaction between the copper(II) and the $\sigma^*(\text{O}_2)$ orbital. Since the σ^* is an antibonding orbital of the peroxide ion, such an interaction should weaken the O–O bond strength, to lower the $\nu(\text{O-O})$.⁴⁶ Although the elongation of the O–O bond distance was not observed experimentally in the X-ray crystal structure of **6**, this theoretical interpretation supports our hypothesis that

(62) Larrabee, J. A.; Spiro, T. G.; Ferris, N. S.; Woodruff, W. H.; Maltese, W. A.; Kerr, M. S. *J. Am. Chem. Soc.* **1977**, *99*, 1979–1980.

(63) Karlin, K. D.; Tyeklar, Z.; Farooq, A.; Haka, M. S.; Ghosh, P.; Cruse, R. W.; Gultneh, Y.; Hayes, J. C.; Zubieta, J. *Inorg. Chem.* Submitted for publication.

(64) XYL-F = α,α' -bis(*N,N*-bis(2-pyridylethyl)aminomethyl)-2-fluoro-*m*-xylylenediamine: Karlin, K. D.; Cruse, R. W.; Haka, M. S.; Gultneh, Y.; Cohen, B. I. *Inorg. Chim. Acta* **1986**, *125*, L43–L44.

(65) tpmc = 1,4,8,11-tetrakis(2'-pyridylmethyl)-1,4,8,11-tetraazacyclo-tetradecane: Asato, E.; Hashimoto, S.; Matsumoto, S.; Kida, S. *J. Chem. Soc., Dalton Trans.* **1990**, 1741–1746.

(66) $\text{DF}_2\text{DIEN}_2 = 3,6,9,16,19,22\text{-hexaazatricyclo}[22.2.1.1^{12,14}]$ octacosal(26),2,9,11,13,15,22,24-octaene: Hgwenya, M. P.; Chen, D.; Martell, A. E.; Reibenspies, J. *Inorg. Chem.* **1991**, *30*, 2732–2736.

(67) $\text{BzN}_3(\text{NMI})_2 = N,N\text{-bis}[2\text{-}(1\text{'-methyl-2'-imidazolyl)ethyl}]\text{-}N\text{-benzylamine}$: Sorrell, T. N.; Garrity, M. L. *Inorg. Chem.* **1991**, *30*, 210–215.

(68) Gubelmann, M. H.; Williams, A. F. *Struct. Bonding (Berlin)* **1983**, *55*, 1–65.

(57) (a) Himmelwright, R. S.; Eickman, N. C.; Solomon, E. I. *J. Am. Chem. Soc.* **1979**, *101*, 1576–1586. (b) Himmelwright, R. S.; Eickman, N. C.; LuBien, C. D.; Solomon, E. I. *J. Am. Chem. Soc.* **1980**, *102*, 5378–5388.

(58) Westmoreland, T. D.; Wilcox, D. E.; Baldwin, M. J.; Mims, W. B.; Solomon, E. I. *J. Am. Chem. Soc.* **1989**, *111*, 6106–6123.

(59) Pate, J. E.; Thamann, T. J.; Solomon, E. I. *Spectrochim. Acta* **1986**, *42A*, 313–318.

(60) Pate, J. E.; Ross, P. K.; Thamann, T. J.; Reed, C. A.; Karlin, K. D.; Sorrell, T. N.; Solomon, E. I. *J. Am. Chem. Soc.* **1989**, *111*, 5198–5209.

(61) Kitajima, N. et al. Unpublished data. Congruence models for met-azide-Hc (containing an alkoxide or phenoxide bridge but not hydroxide) have been reported: (a) McKee, V.; Zvagulis, M.; Dagdigian, J. V.; Patch, M. G.; Reed, C. A. *J. Am. Chem. Soc.* **1984**, *106*, 4765–4772. (b) Sorrell, T. N.; O'Connor, C. J.; Anderson, O. P.; Reibenspies, J. H. *J. Am. Chem. Soc.* **1985**, *107*, 4199–4206.

Table VI. Physicochemical Properties of $\mu\text{-}\eta^2\text{:}\eta^2$ Peroxo Complexes 5-7 and oxy-Hc and oxy-Tyr

	magnetic property	absorption bands/nm (ϵ)	ν (O-O) (cm^{-1})	Cu-Cu (\AA)	ν (C-O) ^a (cm^{-1})
5 ^b	diamag	530 (840), 338 (20800)	731	—	2066
6 ^c	diamag	551 (790), 349 (21000)	741	3.56	2056
7 ^c	diamag	542 (1040), 355 (18000)	759	—	2086
oxy-Hc	diamag ^d	580 (1000), 340 (20000) ^f	744-752 ^h	3.5-3.7 ^j	2043-2063 ^l
oxy-Tyr	diamag ^e	600 (1200), 345 (18000) ^g	755 ⁱ	ca. 3.6 ^k	—

^a ν (CO) is for the corresponding copper(I) carbonyl complex or CO adduct of Hc. ^bReferences 26 and 29. ^cPresent work. ^dReferences 9 and 10. ^eReferences 14 and 73. ^fReferences 1-3. ^gReference 12. ^hReference 7. ⁱReference 13. ^jReferences 41 and 42. ^kReference 43. ^lReferences 50 and 51.

the unusually low O-O stretching frequency is characteristic for the $\mu\text{-}\eta^2\text{:}\eta^2$ structure.

Conclusions

In the present study, by using sterically hindered tris(pyrazolyl)borate ligands, we have succeeded in preparing μ -peroxo dinuclear copper(II) complexes (6 and 7) which show many similarities to oxy-Hc and oxy-Tyr in their physicochemical properties. The complexes were prepared either by the low-temperature reaction of di- μ -hydroxo dicopper(II) complex (8) with H_2O_2 or by the direct addition of dioxygen to copper(I) complexes (9 and 10). An X-ray analysis was successfully applied to 6, which established the $\mu\text{-}\eta^2\text{:}\eta^2$ coordination of the peroxide ion for the first time. This coordination structure is entirely novel for d-block element transition-metal complexes. On the basis of the remarkable physicochemical similarities between the peroxo complexes 5-7 and oxy-Hc and oxy-Tyr, we propose the unusual side-on coordination structure of the peroxide ion, $\mu\text{-}\eta^2\text{:}\eta^2$, as a plausible model for the dioxygen binding structure in these proteins. Although some of the precise assignments of the characteristic properties remain to be solved (further physicochemical investigations including EXAFS, resonance Raman profile experiments, absorption spectroscopy on the solid sample are planned or in progress to ascertain these aspects), it should be emphasized that there is no experimental or theoretical implication which is negative for our proposal. Rather, based on this model for the dioxygen binding in oxy-Hc, the existence of an endogenous bridging ligand is no longer necessary. The existence of a bridging ligand has been discussed for quite some time; however, the nature, or even the existence of the ligand, has never been proven to date. Existence of a bridging ligand in EPR inert met-Hc is evident, but it does not necessarily mean that oxy-Hc contains the same bridging ligand. Thus the proposal should be considered seriously, although the possibility of the cis- μ -1,2 structure with an endogenous bridging ligand, cannot be ruled out completely at the present stage. The synthesis and full characterization of a cis- μ -1,2 peroxo complex with a OH bridge and the comparison of its properties with 5-7 should distinguish these two structural possibilities for oxy-Hc and oxy-Tyr; ultimately a high-resolution X-ray analysis of the proteins will be required for the definitive conclusion.

Experimental Section

Instrumentation. ¹H NMR spectra were recorded on a either JEOL-GX-270 (270 MHz) or JEOL-GX-500 (500 MHz) NMR spectrometer. Chemical shifts were referenced relative to an internal standard Me_4Si . Electronic spectra were recorded on a Shimadzu UV-260 instrument at room temperature. Low-temperature measurements of absorption spectra were carried out on a MRS-2000 spectrometer equipped with a cooling apparatus at Keio University. IR spectra were measured on a Hitachi 260-50 spectrometer by a KBr method. Magnetic susceptibilities were determined by the Evans method⁴⁴ or Faraday method.

Raman scattering was excited by the 514.5-nm line of an Ar⁺ ion laser (NEC GLG3200) with the laser power of 80 mW at the sample point and detected with an OMA II system (PAR 1215) and an intensified diode-array detector (PAR 1420) attached to a double monochromator (Spex 1404). The sample was contained in a spinning cell (diameter = 20 mm, 1000 rpm) and kept at -40 °C by flushing with cold nitrogen gas. The Raman shifts were calibrated with indene.

X-ray data were collected on a Rigaku AFC-5 four-circle diffractometer (AFC program package from Rigaku). A cooling apparatus obtained from Rigaku was used for low-temperature experiments. The structural analyses were completed either by a FACOM A-70 computer with CRYSTAN program package provided from Rigaku or a HITAC

M680H computer with the computation program UNICS-III.⁶⁹

Materials. All reactions were performed under argon by standard Schlenk techniques unless otherwise stated. CHCl_3 and CH_2Cl_2 were carefully purified⁷⁰ and refluxed/distilled under argon prior to use. CuCl (reagent grade) was purchased from Wako and treated with acetic acid on a filter until the filtrate became colorless. The resultant white solid was washed with distilled water and then with ethanol/ether several times and then dried under vacuum. Other reagents were of the highest grade commercially available and used without further purification.

3,5-Diisopropylpyrazole. Phenyl isobutyrate used for the preparation of 3,5-diisopropylpyrazole was synthesized as follows. Isobutyric acid (99.9 g, 1.13 mol), phenol (217.9 g, 2.32 mol), and benzene (200 mL) were refluxed in the presence of concentrated sulfuric acid (2 mL) until ca. 17 mL of water was generated. The solution was washed with aqueous NaOH solution to remove excess phenol and treated with saturated NaCl aqueous solution. The benzene extract was dried over MgSO_4 overnight. After the removal of MgSO_4 by filtration, benzene was evaporated from the solution. Distillation of the resultant solution under reduced pressure afforded 128.2 g of phenyl isobutyrate (69%).

Lithium amide (48.1 g, 2.09 mol) and diethyl ether (800 mL) (pre-purified by distillation) were placed in a 2-L three-necked flask. To the mixture was added dropwise a solution of isopropyl methyl ketone (102.0 g, 1.18 mol) in 60 mL of diethyl ether over a 25-min period. Phenyl isobutyrate (97.6 g, 0.59 mol) dissolved in diethyl ether (150 mL) was then added dropwise to the mixture of a 20-min period. After being refluxed for 8 h, a dilute HCl aqueous solution was added to the mixture to hydrolyze unreacted lithium amide. Subsequently, the mixture was treated with aqueous NaOH to remove a byproduct, phenol, followed by washing with a saturated NaCl aqueous solution several times. After drying over MgSO_4 , diethyl ether was removed by evaporation. The resulting solution was distilled under reduced pressure (at 75 °C, 10 mmHg), affording 78.5 g of diisobutrylmethane (85%).

In a 300-mL three-necked flask, aqueous hydrazine monohydrate (31.0 g, 0.62 mol) was added dropwise to a solution of diisobutrylmethane (63.9 g, 0.41 mol) dissolved in 210 mL of ethanol. After 10 h of refluxing, the mixture was washed with NaOH and NaCl aqueous solution, respectively, to remove unreacted hydrazine and phenol. After being dried over MgSO_4 overnight, the solvent was evaporated to dryness. The resultant white solid was recrystallized from hexane, affording 3,5-diisopropylpyrazole as white needles (25.8 g, 41%): ¹H NMR ($(\text{CD}_3)_2\text{CO}$, 270 MHz) δ 1.24 (d, $J = 7.3$ Hz, 12 H, CHMe_2), 2.93 (m, $J = 7.3$ Hz, 2 H, CHMe_2), 5.86 (s, 1 H, pz), 11.34 (s, br, 1 H, NH). Anal. Calcd for $\text{C}_9\text{H}_{16}\text{N}_2$: C, 71.01; H, 10.59; N, 18.40. Found: 71.04; H, 10.70; N, 18.51.

3,5-Diphenylpyrazole. To a solution of dibenzoylmethane (purchased from Wako) (75.7 g, 0.34 mol) in 150 mL of ethanol, hydrazine monohydrate (20.4 g, 0.41 mol) was added dropwise. The reaction mixture was warmed to ca. 50 °C; at that temperature, benzoylmethane was dissolved and formation of a white crystalline material was noted. Subsequently, the mixture was refluxed for 30 min. The mixture was allowed to cool to room temperature, and the formed white solid was collected by filtration. The recrystallization of the solids from acetone gave 3,5-diphenylpyrazole as white needles (63.7 g, 85%): ¹H NMR ($(\text{CD}_3)_2\text{CO}$, 270 MHz) δ 7.12 (s, 1 H, pz), 7.30-7.50 (m, 6 H, Ph), 7.85-7.95 (m, 4 H, Ph), 12.52 (s, br, 1 H, NH). Anal. Calcd for $\text{C}_{15}\text{H}_{12}\text{N}_2$: C, 81.79; H, 5.49; N, 12.72. Found: C, 82.00; H, 5.49; N, 12.79.

(69) Sakurai, T.; Kobayashi, K. *Rikagaku Kenkyusho Hokoku* 1979, 55, 69-77.

(70) Perrin, D. D.; Armarego, W. L. F.; Perrin, D. R. *Purification of Laboratory Chemicals*; Pergamon: New York, 1980.

(71) Hoffmann, R. *J. Chem. Phys.* 1963, 39, 1397-1412.

(72) Summerville, R. H.; Hoffmann, R. *J. Am. Chem. Soc.* 1976, 98, 7240-7254.

(73) Deinum, J.; Lerch, K.; Reinhammar, B. *FEBS Lett.* 1976, 69, 161-164.

KHB(3,5-*i*-Pr₂p_z)₃, 3,5-Diisopropylpyrazole (15.1 g, 0.10 mol) and KBH₄ (1.66 g, 0.03 mol) were placed in a 200-mL flask. The mixture was warmed gradually while monitoring hydrogen evolution. The temperature was finally elevated to 260 °C, and heating continued until no hydrogen evolution was observed. Almost 3 equiv of hydrogen per KBH₄ was obtained. The mixture was allowed to cool to room temperature, and the resultant pale yellow solid was extracted with CH₂Cl₂. The extract was dried under vacuum, and the resultant solid was carefully recrystallized from pentane, affording KHB(3,5-*i*-Pr₂p_z)₃ as a white crystalline solid (7.48 g, 44%). ¹H NMR ((CD₃)₂CO, 270 MHz) δ 1.01 (d, *J* = 7.3 Hz, 18 H, CHMe₂), 1.08 (d, *J* = 7.3 Hz, 18 H, CHMe₂), 2.76 (m, *J* = 7.3 Hz, 3 H, CHMe₂), 3.18 (m, *J* = 7.3 Hz, 3 H, CHMe₂), 5.73 (3 H, s, pz); IR (KBr, cm⁻¹) 2959 (CH), 2926 (CH), 2865 (CH), 2467 (BH), 1531, 1468, 1379, 1302, 1188, 1172, 1048, 1002, 991, 791, 721, 659. Anal. Calcd for C₂₇H₄₆N₆BK: C, 64.27; H, 9.19; N, 16.65. Found: C, 64.27; H, 9.24; N, 16.68.

KHB(3,5-Ph₂p_z)₃. A mixture of 3,5-diphenylpyrazole (63.1 g, 0.29 mol) and KBH₄ (3.87 g, 0.072 mol) was heated up gradually. At ca. 200 °C, 3,5-diphenylpyrazole was noted to melt with a slight evolution of hydrogen. The mixture was finally heated at 250 °C until 3 equiv of hydrogen per KBH₄ had evolved. The mixture was allowed to cool to ca. 200 °C, and to the hot mixture was added toluene with vigorous stirring. The hot toluene solution was separated by filtration. This treatment was repeated several times to remove unreacted 3,5-diphenylpyrazole. Finally, the remaining solid was washed with hexane to give KHB(3,5-Ph₂p_z)₃ as a white crystalline solid (22.2 g, 33%): ¹H NMR ((CD₃)₂CO, 270 MHz) δ 6.75 (s, 3 H, pz), 6.95–7.50 (m, 18 H, Ph), 7.80–7.95 (m, 12 H, Ph); IR (KBr, cm⁻¹) 3040 (CH), 2527 (BH), 1603, 1546, 1479, 1461, 1447, 1430, 1406, 1341, 1331, 1237, 1177, 1122, 1072, 757. Anal. Calcd for C₄₅H₃₄N₆BK: C, 76.25; H, 4.84; N, 11.86. Found: C, 76.25; H, 5.01; N, 11.88.

[Cu(HB(3,5-*i*-Pr₂p_z)₃)₂(OH)₂ (8). The reaction of CuBr₂ with 1 equiv of KHB(3,5-*i*-Pr₂p_z)₃ in a 1:4 mixture of acetone and CH₂Cl₂ gives brown-colored Cu(Br)(HB(3,5-*i*-Pr₂p_z)₃). The details of the synthesis and properties of this complex will be described elsewhere.⁴⁰ To a solution of Cu(Br)(HB(3,5-*i*-Pr₂p_z)₃) (191 mg, 0.314 mmol) in toluene under argon was added dropwise 15 mL of 1 N aqueous NaOH solution. The color of the deep reddish-brown toluene phase gradually turned to blue. After stirring 1 h, the toluene phase was separated and evacuated to dryness under vacuum. The recrystallization of the resultant solid from CH₂Cl₂ at -20 °C afforded [Cu(HB(3,5-*i*-Pr₂p_z)₃)₂(OH)₂ (8) solvated with CH₂Cl₂ as blue needles (104 mg, 61%). The single crystals of 8·1.5(CH₂Cl₂) suitable for X-ray diffraction were obtained by slow recrystallization from CH₂Cl₂. The crystal contains CH₂Cl₂ of crystallization which is lost easily when the crystal is exposed to air or under vacuum. ¹H NMR (C₆D₆CD₃, 270 MHz, at -40 °C) δ -52 (br, 2 H, OH), 1.25 (s, br, 36 H, CHMe₂), 1.74 (s, br, 36 H, CHMe₂), 3.02 (s, br, 6 H, CHMe₂), 4.51 (s, br, 6 H, CHMe₂), 13.17 (s, br, 6 H, pz); IR (KBr, cm⁻¹) 3645 (OH), 2959 (CH), 2925 (CH), 2863 (CH), 2527 (BH), 1536, 1468, 1391, 1381, 1298, 1174, 1052, 785; UV-vis (CH₂Cl₂, nm (cm⁻¹ M⁻¹)) 260 (6800), 653 (120). Anal. Calcd for C₅₄H₉₄N₁₂O₂B₂Cu₂: C, 59.39; H, 8.68; N, 15.39. Found: C, 59.48; H, 8.86; N, 15.27.

Cu(HB(3,5-*i*-Pr₂p_z)₃)₂ (9). Owing to its high oxygen sensitivity, the preparation of this complex was carried out with carefully dehydrated (with fresh molecular sieves 4Å) and deoxygenated acetone. In a 50-mL Schlenk flask were placed KHB(3,5-*i*-Pr₂p_z)₃ (123 mg, 0.244 mmol) and CuCl (21 mg, 0.212 mmol). Under argon, 5 mL of acetone was added, and the mixture was stirred for 1 h. Filtration, following evaporation to dryness of the colorless filtrate under vacuum, gave a quantitative amount of Cu(HB(3,5-*i*-Pr₂p_z)₃)₂ as a white solid: ¹H NMR (C₆D₆CD₃, 270 MHz) δ 1.28 (d, *J* = 7 Hz, 18 H, CHMe₂), 1.37 (d, *J* = 7 Hz, 18 H, CHMe₂), 3.32 (m, *J* = 7 Hz, 3 H, CHMe₂), 3.71 (m, *J* = 7 Hz, 3 H, CHMe₂), 5.89 (s, 3 H, pz); IR (KBr, cm⁻¹) 2960 (CH), 2926 (CH), 2865 (CH), 2523 (BH), 1537, 1468, 1382, 1300, 1174, 1050, 1048, 786, 653. Anal. Calcd for C₂₇H₄₆N₆B₂Cu: C, 61.30; H, 8.76; N, 15.88. Found: C, 62.05; H, 9.28; N, 15.22.

Cu(Me₂CO)(HB(3,5-Ph₂p_z)₃) (10). To a mixture of KHB(3,5-Ph₂p_z)₃ (1000 mg, 1.41 mmol) and CuCl (150 mg, 1.52 mmol) under argon was added 40 mL of acetone. The mixture was stirred for 3 h and filtered. The volume of the clear yellow filtrate was reduced 2-fold under vacuum and cooled at -20 °C overnight, affording 10 as yellow crystals (720 mg, 65%): ¹H NMR (CD₂Cl₂, 270 MHz) δ 2.08 (s, 6 H, Me), 6.30 (s, 3 H, pz), 6.65–7.15 (m, 24 H, Ph), 7.35–7.50 (m, 6 H, Ph); IR (KBr, cm⁻¹) 3057 (CH(Ph)), 2599 (BH), 1676 (CO), 1477, 1461, 1342, 1160, 758, 693. Anal. Calcd for C₄₈H₄₀N₆OBCu: C, 72.86; H, 5.10; N, 10.62. Found: C, 72.40; H, 5.01; N, 10.22.

[Cu(HB(3,5-*i*-Pr₂p_z)₃)₂(O₂) (6). In an analogous manner applied for the synthesis of [Cu(HB(3,5-Ph₂p_z)₃)₂(O₂), the reaction of 8 with H₂O₂ gave [Cu(HB(3,5-*i*-Pr₂p_z)₃)₂(O₂) (6). In a typical experiment, 316 mg

of 8 (0.29 mmol) was dissolved in 15 mL of CH₂Cl₂. After cooling to -50 °C, 200 μL of H₂O₂ (35 wt % aqueous solution) was added to the solution. The color of the solution gradually turned to deep purple. After stirring for 2 h, the mixture was cooled at -78 °C for 10 min, causing precipitation of 6 solvated with CH₂Cl₂. The purple solid was collected by filtration and dried under vacuum at -20 °C, affording 279 mg of 6 (0.26 mmol, 88% yield). Single crystals of 6·6(CH₂Cl₂) suitable for X-ray diffraction were obtained as follows. Seventy milligrams of 8 was dissolved in 6 mL of CH₂Cl₂ and cooled at -20 °C. Added into the solution was 40 μL of H₂O₂ aqueous solution. The solution was stirred for 1 h at -20 °C and then warmed to 0 °C, being kept for a minute, to dissolve the formed precipitates. Then the deep purple homogeneous solution was cooled overnight at -30 °C, resulting in the single crystals.

The μ-peroxo complex 6 was also prepared by a direct addition of dioxygen to 9. The solution of complex 9 was prepared in situ for this experiment. KHB(3,5-*i*-Pr₂p_z)₃ (190 mg, 0.377 mmol) and CuCl (35 mg, 0.354 mmol) were reacted in 6 mL of acetone as described before, and the colorless filtrate obtained from the mixture was cooled at -78 °C and stirred under 1 atm of dioxygen for 2 h. The resulting deep purple-colored solution was evacuated under vacuum to dryness, affording an almost quantitative amount of 6. ¹H NMR (C₆D₆CD₃, 500 MHz, at -10 °C) δ 1.14 (d, *J* = 6 Hz, 36 H, CHMe₂), 1.33 (d, *J* = 6 Hz, 36 H, CHMe₂), 3.53 (m, *J* = 6 Hz, 6 H, CHMe₂), 3.78 (m, *J* = 6 Hz, 6 H, CHMe₂), 4.17 (s, 12 H, CH₂Cl₂), 5.94 (s, 6 H, pz); IR (KBr, cm⁻¹) 2966 (CH), 2931 (CH), 2870 (CH), 2539 (BH), 1538, 1473, 1460, 1395, 1382, 1301, 1175, 1053, 788, 737 (O-O), 705, 657. The band at 737 cm⁻¹ was not observed for 6 labeled with ¹⁸O. The ν(¹⁸O-¹⁸O) band may be overlapped with a band at 705 cm⁻¹. UV-vis (acetone, at -12 °C, nm (cm⁻¹ M⁻¹)) 349 (21 000), 551 (790); ν(O-O), 741 cm⁻¹ (by resonance Raman with 514.5-nm excitation in acetone at -40 °C); μ_{eff} (Evans method, in C₆D₆CD₃ at -10 °C) 0 μ_B/mol; FD-MSC, *m/z* 1090 (M⁺). Anal. Calcd for C₅₄H₉₂N₁₂O₂B₂Cu₂: C, 59.50; H, 8.51; N, 15.42. Found: C, 58.94; H, 8.54; N, 15.27.

[Cu(HB(3,5-Ph₂p_z)₃)₂(O₂) (7). Sixty-nine milligrams of 10 (0.086 mmol) was dissolved in 3 mL of CH₂Cl₂ and cooled enough at -78 °C under argon. The atmosphere in the Schlenk tube was replaced with 1 atm of dioxygen, and the solution was stirred for 1 h to give a deep purple-colored solution. The independent experiment combined with a closed vacuum/manometric system established that the O₂ uptake at this stage is ca. 0.5 per mol of 10. The solution was allowed to warm to room temperature, causing precipitation of a slightly reddish purple-colored solid of [Cu(HB(3,5-Ph₂p_z)₃)₂(O₂) as a solvate with CH₂Cl₂ (55 mg, 73%), which was collected by filtration and dried under vacuum. The solid complex is reasonably stable even at room temperature. Once this complex is isolated as a solid, it shows only a very low solubility in any solvent we tried, and thus the spectroscopic measurements were accomplished with a solution prepared in situ just before the precipitation began: ¹H NMR (CD₂Cl₂, 500 MHz, at -45 °C) δ 6.34 (s, 6 H, pz), 6.74–6.83 (m, 18 H, Ph), 6.98–7.39 (m, 42 H, Ph); IR (KBr, cm⁻¹) 3058 (CH), 2607 (BH), 1602, 1478, 1461, 1341, 1169; UV-vis (CH₂Cl₂, at -12 °C, nm (cm⁻¹ M⁻¹)) 355 (18 000), 542 (1040); ν(O-O), 759 cm⁻¹ (in CH₂Br₂ at -40 °C); μ_{eff} (Faraday method, at 25 °C) 0 μ_B/mol. Anal. Calcd for 7·3(CH₂Cl₂) (C₉₃H₇₄N₁₂O₂Cl₆B₂Cu₂): C, 63.72; H, 4.25; N, 9.59; Cl, 12.13. Found: C, 64.32; H, 4.36; N 9.67; Cl, 11.88.

Reaction of 6 with CO To Give Cu(CO)(HB(3,5-*i*-Pr₂p_z)₃) (11). In a Schlenk tube, 10 mg of 6 was dissolved in 20 mL of CH₂Cl₂ and cooled at -78 °C under argon. The atmosphere was replaced with CO, and the solution was allowed to warm to room temperature to give a slightly greenish solution. The evaporation of the solvent afforded an almost quantitative amount of Cu(CO)(HB(3,5-*i*-Pr₂p_z)₃) (11). An authentic sample of 11 was obtained by the reaction 9 and CO. The crystals suitable for X-ray experiments were grown by slow recrystallization from acetone. ¹H NMR (CD₂Cl₂, 270 MHz) δ 1.21 (d, *J* = 7 Hz, 18 H, CHMe₂), 1.26 (d, *J* = 7 Hz, 18 H, CHMe₂), 3.05 (m, *J* = 7 Hz, 3 H, CHMe₂), 3.41 (m, *J* = 7 Hz, 3 H, CHMe₂), 5.82 (s, 3 H, pz); IR (KBr, cm⁻¹) 2957 (CH), 2926 (CH), 2862 (CH), 2525 (BH), 2056 (CO), 1534, 1469, 1397, 1381, 1300, 1169, 1046, 786. Anal. Calcd for C₂₈H₄₆N₆OBCu: C, 60.37; H, 8.32; N, 15.09. Found: 60.09; H, 8.21; N, 15.00.

Cu(PPh₃)(HB(3,5-*i*-Pr₂p_z)₃) (12). The reaction of 6 with 5 equiv of PPh₃ at -20 °C gave a quantitative amount of Cu(PPh₃)(HB(3,5-*i*-Pr₂p_z)₃) (12). An authentic sample of 12 was obtained by the reaction of in situ prepared 9 and PPh₃. The filtrate, obtained from the reaction mixture of HB(3,5-*i*-Pr₂p_z)₃ (224 mg, 0.443 mmol) and CuCl (40 mg, 0.403 mmol) stirred for 1 h in 8 mL of acetone, was treated with a solution of PPh₃ (233 mg, 0.857 mmol) in 10 mL of diethyl ether. After stirring overnight, the volume of the solution was reduced by ca. half and cooled at -20 °C. White needles were formed, which were collected by filtration and dried under vacuum (95 mg, 30%): ¹H NMR ((CD₃)₂CO, 270 MHz) δ 0.73 (d, *J* = 7 Hz, 18 H, CHMe₂), 1.27 (d, *J* = 7 Hz, 18

Table VII. Crystallographic Data for

[Cu(HB(3,5-*i*-Pr₂pz)₃)₂(O₂)-6(CH₂Cl₂)] (6-6(CH₂Cl₂)),
 [Cu(HB(3,5-*i*-Pr₂pz)₃)₂(OH)₂-1.5(CH₂Cl₂)] (8-1.5(CH₂Cl₂)),
 Cu(CO)(HB(3,5-*i*-Pr₂pz)₃) (11)

6-6(CH ₂ Cl ₂)	
C ₆₀ H ₁₀₄ N ₁₂ B ₂ Cl ₁₂ Cu ₂	monoclinic, C2/c
<i>a</i> = 26.36 (2) Å	μ(Mo Kα) = 7.98 cm ⁻¹
<i>b</i> = 13.290 (4) Å	<i>T</i> _m = -75 °C
<i>c</i> = 29.29 (2) Å	2° ≤ 2θ ≤ 45°
β = 114.59 (6)°	no. of measd reflns = 9740
<i>V</i> = 7915 (9) Å ³	no. of independent reflns = 3003
<i>Z</i> = 4	<i>D</i> _c = 1.34 g cm ⁻³
fw = 1599.71	<i>R</i> = 0.101
	<i>R</i> _w = 0.148
8-1.5(CH ₂ Cl ₂)	
C _{55.5} H ₉₇ N ₁₂ O ₂ B ₂ Cl ₃ Cu ₂	triclinic, P1̄
<i>a</i> = 16.466 (4) Å	μ(Mo Kα) = 6.01 cm ⁻¹
<i>b</i> = 16.904 (5) Å	<i>T</i> _m = -75 °C
<i>c</i> = 14.077 (3) Å	2° ≤ 2θ ≤ 50°
α = 112.92 (2)°	no. of measd reflns = 12 080
β = 99.21 (2)°	no. of independent reflns = 7226
γ = 90.76 (2)°	<i>D</i> _c = 1.14 g cm ⁻³
<i>V</i> = 3550 (2) Å ³	<i>R</i> = 0.083
<i>Z</i> = 2	<i>R</i> _w = 0.105
fw = 1219.54	
11	
C ₂₈ H ₄₆ N ₆ O ₁ B ₁ Cu ₁	monoclinic, P2 ₁ /a
<i>a</i> = 16.595 (4) Å	μ(Mo Kα) = 6.78 cm ⁻¹
<i>b</i> = 19.154 (4) Å	<i>T</i> _m = 25 °C
<i>c</i> = 10.359 (2) Å	3° ≤ 2θ ≤ 55°
β = 106.65 (2)°	no. of measd reflns = 7983
<i>V</i> = 3155 (1) Å ³	no. of independent reflns = 5356
<i>Z</i> = 4	<i>D</i> _c = 1.17 g cm ⁻³
fw = 557.08	<i>R</i> = 0.083
	<i>R</i> _w = 0.074

H, CHMe₂, 2.79 (m, *J* = 7 Hz, 3 H, CHMe), 3.62 (m, *J* = 7 Hz, 3 H, CHMe₂), 5.82 (s, 3 H, pz), 7.2–7.8 (m, 15 H, PPh₃); IR (KBr, cm⁻¹) 3054 (CH(Ph)), 2957 (CH), 2923 (CH), 2862 (CH), 2526 (BH), 1536, 1469, 1436, 1393, 1380, 1296, 1170, 791. Anal. Calcd for C₄₅H₆₁N₆BPCu: C, 68.30; H, 7.77; N, 10.62. Found: C, 67.96; H, 8.08; N, 10.52.

Cu(CO)(HB(3,5-Ph₂pz)₃) (13). The suspension of 7 in CH₂Cl₂ was stirred in a Schlenk flask under 1 atm of CO for a week. An almost colorless homogeneous solution was obtained. Evaporation of the solution yielded an almost quantitative amount of Cu(CO)(HB(3,5-Ph₂pz)₃) (13). An authentic sample of 13 was prepared as follows; CuCl (4.78 mmol, 473 mg) and 2960 mg of KHB(3,5-Ph₂pz)₃ (4.18 mmol) were stirred under 1 atm of CO for 6 h. Filtration gave a colorless filtrate which was evacuated to dryness. Recrystallization of the resulting white solid from CH₂Cl₂ afforded 13 as a microcrystalline white solid (2650 mg, 83%): ¹H NMR (CD₂Cl₂, 270 MHz) δ 6.49 (s, 3 H, pz), 6.9–7.9 (m, 30 H, Ph); IR (KBr, cm⁻¹) 3043 (CH(Ph)), 2635 (BH), 2086 (CO), 1605, 1542, 1476, 1458, 1431, 1414, 1362, 1341, 1313, 1280, 1167. Anal. Calcd for C₄₆H₃₄N₆OBCu: C, 72.59; H, 4.50; N, 11.04. Found: C, 71.98; H, 4.21; N, 11.18.

X-ray Data Collection. The X-ray data collection for 6-6(CH₂Cl₂) and 8-1.5(CH₂Cl₂) were carried out at -75 °C. Because of the rapid loss of the crystallinity at room temperature, the mounting and sealing of the crystal in a glass capillary was performed at low temperature. The crystal of 11 was also sealed in a glass capillary, but the data collection was completed at room temperature. Graphite-monochromated Mo Kα radiation (λ = 0.71068 Å) was used as the X-ray source. Automatic centering and least-squares routines were carried out for all the complexes to determine the cell parameters with 25 reflections (25° ≤ 2θ ≤ 30°). All data were corrected for Lorentz and polarization effects but not for absorption. Intensities of three check reflections monitored every 100 reflections did not show any decay in each experiment. A summary of cell dimensions, details of data collection, and refinement results for 6-6(CH₂Cl₂), 8-1.5(CH₂Cl₂), and 11 are given in Table VII.

Structural Determinations. The computer-programmed automatic cell determination established the crystal system of 6-6(CH₂Cl₂) as triclinic: *a* = 12.975 (4) Å, *b* = 27.473 (7) Å, *c* = 12.941 (5) Å, α = 98.83 (3)°, β = 118.31 (2)°, γ = 95.39 (3)°, *V* = 3939 (2) Å³. The data were

collected based on these cell dimensions. With the space group choice of P1, the initial crystal structure was solved by the Patterson method and subsequent difference Fourier syntheses. The refinement converged at the *R*(*R*_w) factor of 0.115 (0.156) with 5945 reflections (*F*_o ≥ 3σ(*F*_o)). The crystal structure consisted of two essentially identical, independent molecules both of which were centrosymmetric. However, this structure was found to be incorrect. The space group could be transformed to C2/c: the coordinate transformations are *x*' = 1/2(*x* + *y* - *z*), *y*' = 1/2(*x* - *y* + *z*), *z*' = *y*. The wrong choice of P1̄ was evident, since pairs of atoms in the two molecules agree closely with the symmetry of C2/c, and the strongest reflections showed excellent agreement in their intensities between related pairs. Furthermore, reflections required to be absent because of the *c*-glide plane were either missing or extremely weak. In fact, the crystal structure was solved successfully based on the space group of C2/c, and the refinement converged with the slightly improved *R*(*R*_w) factor as shown in Table VII. Now only one molecule is crystallographically independent, which is more reasonable than the initial solution. In these calculations, block-diagonal least-squares were applied with UNICS-III.⁶⁹ All non-hydrogen atoms were included in the refinement of anisotropic thermal parameters, and the hydrogens with the exception of those on the methyl groups and CH₂Cl₂ molecules were calculated and fixed for the final refinements. The slightly higher residual values are presumably due to the deterioration of the crystallinity during the mounting of the crystal, positional disorders of CH₂Cl₂ molecules, and thus the essentially low crystallinity of 6-6(CH₂Cl₂). Two other data collections of the X-ray data were carried out, but unfortunately no improvement in the structural refinement was gained because of the low quality of the data.

The positional parameters for the copper atoms in 8-1.5(CH₂Cl₂) and 11 were determined by the direct method (SAPI 85 provided by Rigaku). Subsequent difference Fourier syntheses located all non-hydrogen atoms easily. Significant disorders of the CH₂Cl₂ of crystallization in 8-1.5(CH₂Cl₂) were found in the difference maps. All non-hydrogen atoms were included for the refinements with anisotropic thermal parameters. The hydrogen atoms on the borons, pyrazole rings, and the methyne positions of the isopropyl groups were calculated and fixed for the final refinements with isotropic thermal parameters (*d*(C-H), 1.0 Å). The other hydrogen atoms were not included for the calculations. The block-diagonal least-squares refinement was applied with UNICS-III for 8-1.5(CH₂Cl₂). The structure of 11 was refined by full-matrix least-squares method with CRYSTAN. The final *R* and *R*_w values and refinement data are summarized in Table VII.

Molecular Orbital Calculations. All the calculations were of the extended Hückel type.⁷¹ The atomic parameters for Cu were taken from previous work as follows:⁷² *H*_{ij}, Cu 4s, -11.4 eV; Cu 4p, -6.06 eV; Cu 3d, -14.0 eV; orbital exponents Cu 4s, 2.2; Cu 4p, 2.2; Cu 3d, 5.95 (0.5933) + 2.30 (0.5744). The C, N, O, and H parameters are the standard ones. The modified Wolfsberg-Helmholz formula for *H*_{ij} was used throughout. The geometrical parameters not specified in the text are as follows: NH₃ group, tetrahedral; N-H, 1.0 Å; [(NH₃)₄Cu₂]₂(O₂)²⁺ Cu-N, 1.95 Å; Cu(N_{equatorial})₃ portion, planar; N_{equatorial}-Cu-N_{equatorial}, 120°; CuO(μ-η²:η² O₂) 1.91 Å. All the O-O distances are fixed at 1.41 Å.

Acknowledgment. We thank Prof. Y. Ishimura, Dr. R. Makino, and Dr. Y. Watanabe of Keio University for low-temperature measurements of electronic spectra. We are grateful for the kind suggestion on the choice of the space group in the X-ray analysis of 6-6(CH₂Cl₂) by a reviewer and Prof. S. J. Lippard of Massachusetts Institute of Technology. This research was supported in part by the Ministry of Education, Science and Culture, Japan (62430018 and 01607003), for which we are grateful. N. Kitajima acknowledges financial support from the Kawakami Memorial Foundation and stimulating discussions by Professors E. I. Solomon (Stanford University) and J. S. Loehr, T. M. Loehr, and N. J. Blackburn (Oregon Graduate Institute of Science and Technology). Finally, we appreciate the kind editing of this manuscript by Dr. J. K. Bashkin of Washington University.

Supplementary Material Available: Tables of crystal data, atomic coordinates and temperature factors, hydrogen coordinates, and intramolecular bond distances and angles (32 pages); tables of observed and calculated structure factors for 6-6(CH₂Cl₂), 8-1.5(CH₂Cl₂), and 11 (34 pages). Ordering information is given on any current masthead page.